Chalcones as positive allosteric modulators of α7 nicotinic acetylcholine receptors: A new target for a privileged structure

ARTICLE *in* EUROPEAN JOURNAL OF MEDICINAL CHEMISTRY · SEPTEMBER 2014

Impact Factor: 3.45 · DOI: 10.1016/j.ejmech.2014.09.039 · Source: PubMed

18 AUTHORS, INCLUDING:

José Mulet
Universidad Miguel Hernández de Elche
32 PUBLICATIONS **485** CITATIONS
SEE PROFILE

Antonio Ferrer Montiel
Universidad Miguel Hernández de Elche
85 PUBLICATIONS **1,872** CITATIONS
SEE PROFILE

Ricardo Borges
Universidad de La Laguna
101 PUBLICATIONS **1,688** CITATIONS
SEE PROFILE

Manuela G López
Universidad Autónoma de Madrid
193 PUBLICATIONS **3,866** CITATIONS
SEE PROFILE

European Journal of Medicinal Chemistry 86 (2014) 724–739

Contents lists available at ScienceDirect

European Journal of Medicinal Chemistry

journal homepage: http://www.elsevier.com/locate/ejmech

Original article

Chalcones as positive allosteric modulators of α7 nicotinic acetylcholine receptors: A new target for a privileged structure

Beatriz Balsera [a], José Mulet [b], Asia Fernández-Carvajal [c], Roberto de la Torre-Martínez [c], Antonio Ferrer-Montiel [c], José G. Hernández-Jiménez [d], Judith Estévez-Herrera [d], Ricardo Borges [d], Andiara E. Freitas [e], Manuela G. López [e], M. Teresa García-López [a], Rosario González-Muñiz [a], María Jesús Pérez de Vega [a], Luis M. Valor [b], Lucie Svobodová [b], Salvador Sala [b], Francisco Sala [b], Manuel Criado [b, *]

[a] Instituto de Química Médica (IQM-CSIC), Juan de la Cierva 3, 28006 Madrid, Spain
[b] Instituto de Neurociencias, Universidad Miguel Hernandez-CSIC, Ramon y Cajal s/n, 03050 Sant Joan d'Alacant, Spain
[c] Instituto de Biología Molecular y Celular, Universidad Miguel Hernandez, Av. de la Universidad s/n, 03202 Elche, Spain
[d] Departamento de Farmacología, Universidad de La Laguna, La Cuesta s/n, 38200 La Laguna, Tenerife, Spain
[e] Instituto Teófilo Hernando, Departamento de Farmacología, Universidad Autónoma de Madrid, Arzobispo Morcillo 4, 28029 Madrid, Spain

ARTICLE INFO

Article history:
Received 22 July 2014
Received in revised form
9 September 2014
Accepted 11 September 2014
Available online

Keywords:
α7 Nicotinic receptor
Positive allosteric modulators
Chalcones
Neuroprotection
Analgesia

ABSTRACT

The α7 acetylcholine nicotine receptor is a ligand-gated ion channel that is involved in cognition disorders, schizophrenia, pain and inflammation among other diseases. Therefore, the development of new agents that target this receptor has great significance. Positive allosteric modulators might be advantageous, since they facilitate receptor responses without directly interacting with the agonist binding site. Here we report the search for and further design of new positive allosteric modulators having the relatively simple chalcone structure. From the natural product isoliquiritigenin as starting point, chalcones substituted with hydroxyl groups at defined locations were identified as optimal and specific promoters of α7 nicotinic function. The most potent compound (2,4,2′,5′-tetrahydroxychalcone, **111**) was further characterized showing its potential as neuroprotective, analgesic and cognitive enhancer, opening the way for future developments around the chalcone structure.

1. Introduction

Nicotinic acetylcholine receptors (nAChRs) modulate fast synaptic transmission in muscle and nerve cells. They exist as pentamers with a variety of pharmacological and electrophysiological properties, mainly due to the various combinations of subunits [1]. In neurons, twelve subunits (α2–α10 and β2–β4) have been identified and cloned. Functional nAChRs can be observed in heterologous expression systems as a result of heteromeric or homomeric assembly of subunits [2]. Within the latter, nAChRs made of only α7 subunits have received much attention, given their widespread distribution at the central and peripheral nervous systems and their characteristic features, different of other neuronal nAChRs, such as rapid channel activation and inactivation kinetics, marked sensitivity to certain agonists (choline) and antagonists (α-bungarotoxin, methyl-lycaconitine) and high Ca^{2+} permeability [3]. The latter property suggests the involvement of α7 nAChRs in processes beyond their channel activity.

Given that α7 nAChRs appear to be engaged in central and peripheral diseases that involve, among others, cognition disorders [4,5], schizophrenia [6], pain [7] and inflammation [8], there has been considerable interest in developing therapeutic agents able to target this receptor subtype. In this context, ligands that facilitate agonist-induced responses but avoid direct interaction with the acetylcholine (ACh) binding site are advantageous, as they should not interfere with the action of the natural agonist on the different nAChR subtypes and are less likely to promote desensitization or downregulation. These positive allosteric modulators (PAMs) selective for α7 nAChRs have a variety of structures, from calcium ions [9] and small molecules [10] to proteins [11]. They also have diverse

Abbreviations: ACh, acetylcholine; α-Bgt, α-bungarotoxin; CFA, complete Freund's adjuvant; DMEM, Dulbecco's modified eagle's medium; MTT, 3-(4,5-dimethylthiazol-2-yl)-2,5-diphenyl-2*H*-tetrazolium bromide; nAChR, nicotinic acetylcholine receptor; PAM, positive allosteric modulator; R/O, rotenone and oligomycin-A.

* Corresponding author.
E-mail address: manuel.criado@umh.es (M. Criado).

http://dx.doi.org/10.1016/j.ejmech.2014.09.039
0223-5234/

potency, efficacy and influence on kinetics of agonist-evoked responses [12,13]. Two large groups of PAMs have been proposed. Those belonging to group I increase the apparent peak current but do not largely modify the kinetics of agonist–mediated responses. Galantamine, 5-hydroxyindole, genistein and ivermectin are representative type I PAMs. PAMs belonging to group II increase the peak current amplitude and slow the desensitization kinetics. Representative compounds of this type are PNU-120596, TQS, and A-867744 (Fig. 1).

In spite of the advantages of PAMs, caution is needed in using them as therapeutic agents to treat the disorders mentioned above. This is mainly due to the high calcium permeability of α7 nAChRs that in certain cases of excessive and/or sustained receptor activation could produce unwanted and even deleterious effects. Therefore, it is important to continue the development of new compounds that, apparently, might have characteristics similar to previous ones, but can make available novel structures with therapeutical potential. With this aim we started the screening of a library of small natural molecules looking for PAMs of different nAChR subtypes heterologously expressed in *Xenopus laevis* oocytes. A flavonoid with a chalcone structure, isoliquiritigenin (4,2′,4′-trihydroxychalcone), showed activity as specific PAM of α7 nAChRs. This chalcone, present in plants like *Glycyrrhiza* and *Dalbergia*, has revealed activities against inflammatory [14], oxidative [15], allergic [16] and carcinogenic [17,18] processes. Also, neuroprotective effects have been reported [19,20]. Given the relevance of α7 nAChRs in some of these processes, we decided to perform a further study of a collection of commercial chalcones differently substituted, which allowed us to refine the molecular requirements for α7 nAChR activation. Finally, the study of our own synthesized compounds defined the position and substituents required for optimal receptor activation. The chalcone with maximal activity was then tested in different systems, showing its potential as neuroprotective, analgesic and learning enhancer.

2. Results and discussion

2.1. Screening of a library of natural compounds and a collection of synthetic chalcones

The Greenpharma Natural compound library (Prestwick Chemical, France), composed of 240 natural compounds of small size, was tested. To speed up the screening, fifty six pools of 4–5 different compounds each were coapplied with ACh (10 μg/mL of each compound and 200 μM ACh) to oocytes expressing either homomeric α7 or heteromeric (α4β2 and α3β4) nAChRs. Currents were measured and compared with the ones induced only by ACh. For α7 nAChRs only one pool showed significant current increases (about 3-fold) respect to controls, whereas no current potentiation was observed for α4β2 and α3β4 nAChRs. Components of the positive pool were individually analyzed as previously and a substance, isoliquiritigenin, was identified as a specific PAM of α7 nAChRs and named **1** in further analysis (Fig. 2). Compound **1** is a polyhydroxy substituted chalcone (Fig. 2a)) that enhanced the current evoked by ACh with little modification of its rising time course, but showing a slower decay time course (Fig. 2b)). The effect of **1** is dose-dependent with an EC_{50} of 11.6 μM and a maximal activation of 6.5-fold about the current induced by 200 μM ACh, a concentration that is close to the EC_{50} (Fig. 2c)). The potentiating effect of **1** was observed throughout a wide range of ACh concentrations (Fig. 2d)), but not in the absence of agonist, indicating that **1** is not acting as agonist itself.

In our search for α7 nAChR PAMs, the chalcone scaffold was further explored with a collection of one hundred differently substituted chalcones from a commercial source. As in the case of **1**, each compound was individually tested by co-application with ACh to α7 nAChRs (see Table S1, supplementary data). Six compounds (**64**, **87**, **97**, **98**, **99**, **101**) showed activity as PAMs and were further characterized. As discussed later in more detail, these compounds have, at least, one OH group in ring A (See Table 1 heading formula), but preferentially two OHs at positions 2′,4′ or 2′,5′. The most effective was **97** (4,2′,5′-OH), about five-fold more than **1**. Its only chemical difference with respect to **1**, is the presence of a hydroxy substitution at the 5′ position instead of the 4′ one.

2.2. Neurosecretory effects of compound **97** on adrenal chromaffin cells

Before continuing the search for compounds with improved properties, we decided to test **97** in a cellular system where cholinergic stimulation gives rise to a clearly measurable biological response. For this purpose, the chromaffin cell of the bovine adrenal medulla is very appropriate, since ACh activates nAChRs triggering catecholamine secretion, which can be amperometrically detected. In our case, choline was used instead, in order to specifically activate α7 nAChRs and not the nAChR responsible of the main cholinergic response in bovine chromaffin cells, which is the one composed of α3, β4 and probably α5 subunits [21].

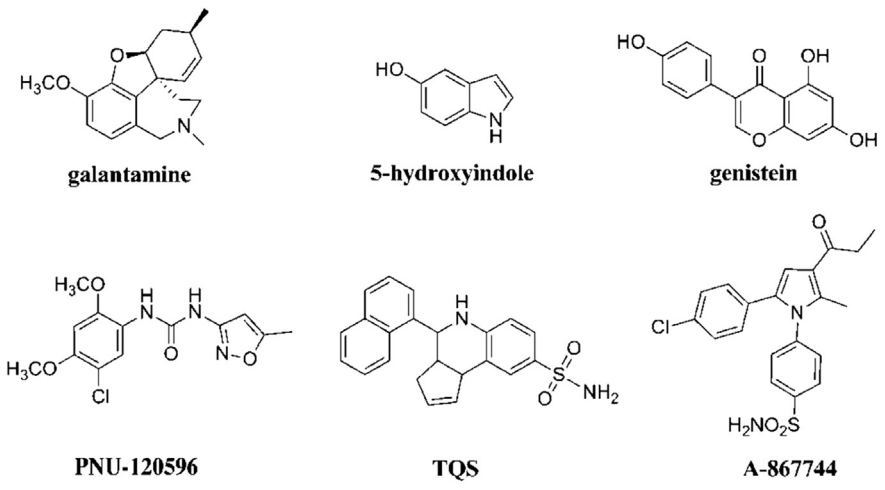

Fig. 1. Chemical structures of representative PAMs of α7 nAChRs. Type I and type II PAMs are shown at the upper and lower rows, respectively.

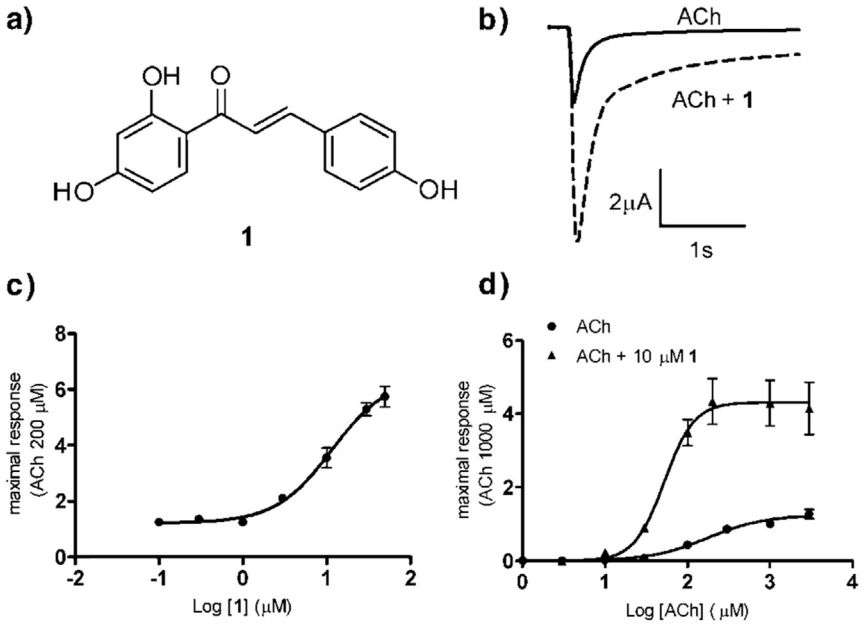

Fig. 2. Effect of compound **1** on α7 nAChRs. a) Chemical structure of compound **1**. b) Ionic currents recorded in a representative oocyte expressing human α7 nAChRs. Currents were evoked by 600 ms applications of ACh 200 μM in the absence (continuous line) and in the presence (dotted line) of 10 μM of **1** and recorded at a holding potential of −80 mV. c) Concentration–response relationship for the potentiating effect of **1** with ACh 200 μM. Continuous line represents the fit to the Hill equation, with a maximal potentiating effect estimated at 6.5, and an EC_{50} value of 11.6 μM d) Acetylcholine concentration–response relationships in the absence (circles) and in the presence (triangles) of 10 μM of **1**. All data were normalized to the response obtained by ACh 1 mM in control conditions. Continuous lines represent fits to Hill equations, with estimated I_{max} of 1.3 and 4.3, and EC_{50} values of 176 μM and 52 μM, for control and compound **1**, respectively.

Fig. 3 shows the effect of compound **97** on the secretory responses elicited by choline. As expected, the application of this α7 agonist produced modest secretory responses when compared to the one observed upon K^+ depolarization (Fig. 3a)). Nevertheless, 10 min incubation with **97** largely increased the catecholamine output elicited by choline. In order to study in detail the effects of **97** in the exocytotic process, we used single cell amperometry. Fig. 3b) shows a typical recording of an amperometrical trace resulting of choline application in the presence of 30 μM of **97**. A large increase in the number of secretory spikes was observed and consequently the secretory response became larger (Fig. 3c)). Thus, it is evidenced that **97** enhances the function of α7 nAChRs in a cellular system.

2.3. Synthesis of new chalcone derivatives

Except for the presence of a methyl group at position 2′ in **64**, the rest of tested substituents in ring A were inefficient for the potentiating function of chalcones (Table S1). In fact, most of the chalcone PAMs contained hydroxy and, to a lesser degree, methoxy substituents. For this reason, we decided to analyze the effect of the number and position of hydroxy substituents of chalcones on their PAM function. With this aim, new compounds were synthesized. Taking the best compounds from the initial screening as the starting point, we prepared a small collection of hydroxychalcone derivatives differently substituted in rings A, B (See Table 1 heading formula) or both. Additionally, to confirm the importance of the hydroxy groups of ring B, some chalcones bearing amino or acetylamino groups in position 4 were also synthesized. Finally, the incorporation of a 5-hydroxyindol moiety replacing ring B was also contemplated in order to compare with the corresponding phenyl derivative.

The preparation of the methoxy substituted chalcones (1,3-diaryl-2-propen-1-ones) **104**–**110** was achieved by the conventional Claisen–Schmidt aldol condensation of the desired benzaldehyde and acetophenone in EtOH using aqueous NaOH (40%) as base [22]. The methoxy substituted chalcones were obtained in moderate to excellent yield (41–87%) (Scheme 1). In the referred condensation conditions, the formation of the *E* isomer as a unique product was observed in all cases, as shown by the NMR data. Demethylation of the methoxy substituted compounds was accomplished by treatment with BBr_3 in DCM under inert atmosphere, which led to the polyhydroxylated analogues after purification (Scheme 1) [23]. As described by McOmie et al., the amount of BBr_3 equivalents necessary for completing the deprotection depends on the number of methyl ether groups to be deprotected. They used at least 1 equiv for each -OMe group, and recommended one extra equiv for every potentially basic N or O present in the molecule [23]. In our case, when using the recommended amount of BBr_3, semideprotected products were isolated. For instance, compound **104** led to formation of the desired tetrahydroxy chalcone **111**, but the partially deprotected compound **112** was also isolated. For compound **105** the use of 6 equiv of BBr_3 led to the isolation of partially deprotected compounds **113** and **114**, while the totally deprotected derivative was never isolated, not even using 12 equiv of the reagent. Based on these initial results, the use of 2 equiv of BBr_3 for each –OMe, O or N present in the molecule was decided, in an attempt to obviate this partial deprotection problem. Using the modified conditions, compounds **106**, **107** and **108** led to the desired **115**, **116** and **117**, respectively, in moderate yields (Scheme 1).

Attempts to prepare the chalcones monohydroxy substituted in ring A, through the preparation of the corresponding *m*- and *p*-OMe derivatives **109**–**110** and further deprotection, failed to lead to the desired OH compounds. In all cases, complex mixtures were obtained in which the desired compounds were not identified. The direct condensation of the 2,4-dihydroxybenzaldehyde with the corresponding monohydroxy substituted acetophenone using

Table 1
Structures of synthetic chalcones and their potentiation of α7 nAChR currents.[a]

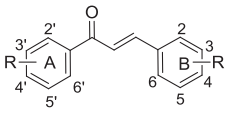

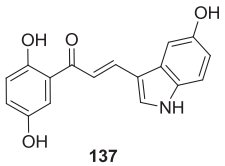

137

Entry	Compd[b]	2	3	4	5	6	2′	3′	4′	5′	6′	I_{max}[c]	EC_{50} (μM)[c]
1	**22**	OH	H	H	H	H	OH	H	H	H	H	–	–
2	**23**	H	OH	H	H	H	OH	H	H	H	H	–	–
3	**24**	H	H	OH	H	H	OH	H	H	H	H	–	–
4	**25**	H	H	H	H	H	OH	H	OH	H	H	–	–
5	**26**	H	H	H	H	H	OH	H	H	OH	H	–	–
6	**98**	OH	H	H	H	H	OH	H	OH	H	H	2.6 ± 0.18	4 ± 0.9
7	**99**	OH	H	H	H	H	OH	H	H	OH	H	3.4 ± 0.24	1.9 ± 0.4
8	**1**	H	H	OH	H	H	OH	H	OH	H	H	6.5 ± 0.8	11.6 ± 1.4
9	**97**	H	H	OH	H	H	OH	H	H	OH	H	33 ± 9.6[d]	25 ± 2.8[d]
10	**96**	H	H	H	H	H	OH	OH	OH	H	H	–	–
11	**125**	OH	H	OH	H	H	OH	H	H	H	H	19.7 ± 6.1	34.5 ± 2.2
12	**126**	OH	H	OH	H	H	H	OH	H	H	H	9 ± 0.9	6.1 ± 1.3
13	**127**	OH	H	OH	H	H	H	H	OH	H	H	8.1[d]	38[d]
14	**111**	OH	H	OH	H	H	OH	H	H	OH	H	34 ± 5.5	3.3 ± 1.6
15	**115**	OH	H	H	H	H	OH	H	OH	OH	H	3.2 ± 0.24[d]	8.9[d]
16	**117**	OH	H	H	H	OH	OH	H	H	OH	H	–	–
17	**101**	H	H	OH	H	H	OH	H	OH	H	OH	2.8 ± 0.15	4 ± 1.3
18	**116**	OH	H	OH	H	H	OH	H	OH	OH	H	14.5 ± 0.3	67 ± 7.1
19	**100**	H	OH	OH	H	H	OH	H	OH	H	OH	–	–
20	**123**[e]	OH	H	OH	H	H	H	H	OH	H	H	–	–
21	**122**[e]	OH	H	OH	H	H	H	H	H	OH	H	11.9 ± 2.1	5.4 ± 1.5
22	**138**[e]	OH	H	OH	H	H	OH	H	H	OH	H	2.3 ± 0.2	10.7 ± 1.6
23	**64**[f]	H	OCH_3	OCH_3	OCH_3	H	CH_3	H	OH	H	H	2.1 ± 0.32	7.3 ± 1.4
24	**87**[f]	H	OCH_3	OH	H	H	OH	H	H	OH	H	6.5 ± 0.4	17.2 ± 1.9
25	**112**[f]	OCH_3	H	OCH_3	H	H	OH	H	H	OH	H	8.6 ± 1.6	3.9 ± 1.4
26	**113**[f]	OH	H	OCH_3	H	OCH_3	OH	H	H	OH	H	7.8 ± 0.52	2.6 ± 1.2
27	**114**	OH	H	OCH_3	H	OH	OH	H	H	OH	H	–	–
28	**133**	H	H	NHAc	H	H	OH	H	H	OH	H	–	–
29	**134**	H	H	NH_2	H	H	OH	H	H	OH	H	–	–
30	**137**	5-OH-indole					OH	H	H	OH	H	3 ± 0.2	1.9 ± 1.3

[a] The substituents 2 to 6 and 2′ to 6′ refer to the positions indicated at the chalcone structure shown above.
[b] Compounds named with numbers **22**-**101** originated from the first screening of commercial chalcones (see Table S1, Supplementary data), whereas the rest (**111**-**138**) were synthesized by us.
[c] Values derived from the corresponding dose response curves. Responses were recorded at −80 mV and normalized with respect to that shown by only ACh (0.2 mM). Data are the mean ± SD, with $n \geq 6$.
[d] Extrapolated values, as no response saturation could be reached because low solubility at higher concentrations.
[e] Compounds **123**, **122** and **138** are *Z*-isomers of compounds **127**, **126** and **111** respectively.
[f] These compounds are the only ones with some substituents different from hydroxyls that showed activity as PAMs.

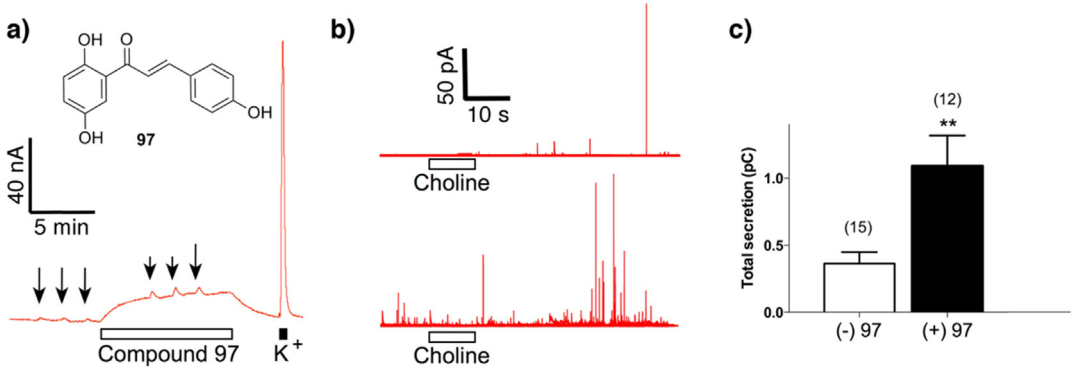

Fig. 3. Compound **97** potentiated the secretory responses triggered by choline. a) Thirty-second applications of the α7 agonist choline (100 μM, arrows) were used to test the effects of **97** (30 μM) (see inset for chemical structure) in perifused bovine chromaffin cells recorded by on-line electrochemical detection. A final 30 s pulse of 70 mM high potassium solution (K^+) was applied at the end of the experiment to assure the cell responsiveness. b) The amperometrical measurements confirmed that the increase in the total release was due to an increase in the number of secretory spikes (compare upper and lower parts of this panel, without and with compound **97**, respectively) rather than to an increase of individual net charge. Each spike of oxidation trace came from single exocytotic events. c) Cumulative secretion from experiments as described in b) are summarized with means ± SEM. $^{**}p < 0.01$ Student *t* test. The number of cells used on each condition is expressed in parentheses.

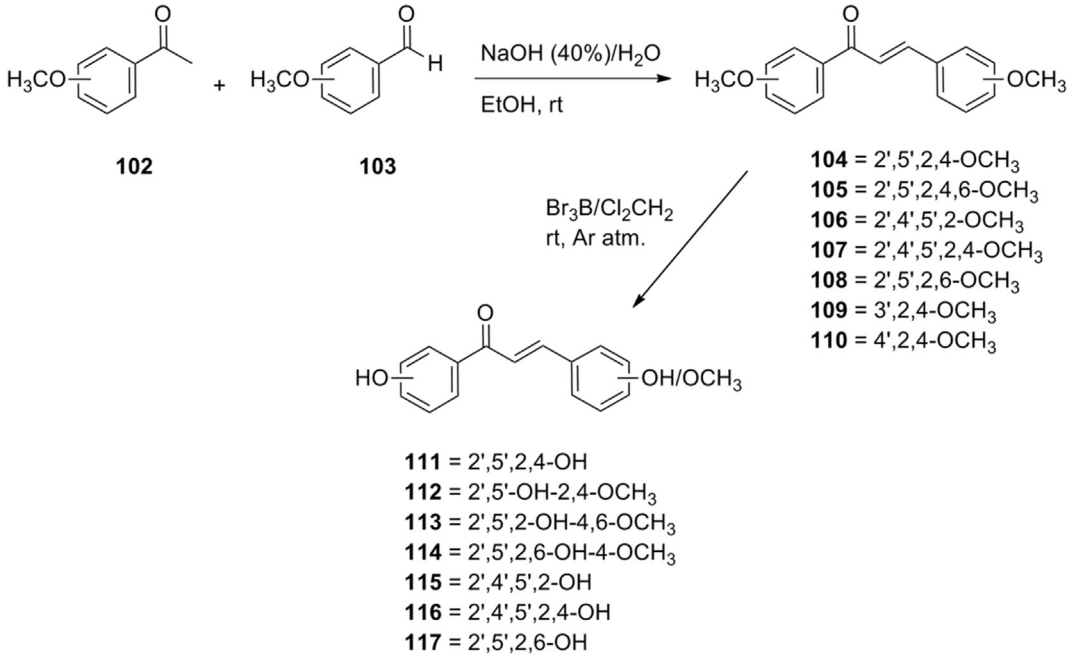

Scheme 1.

different reagents and conditions also failed to lead to the expected polyhydroxylated compounds. The use of $Ba(OH)_2 8H_2O$ [24] as an alternative to NaOH as base, as well as the acid catalysis with Lewis acids ($Yb(OTf)_3$, $AlCl_3$) [25] was also tried without success. Only when $F_3B{\cdot}Et_2O$ was used as reagent, the condensation product was isolated [26]. This procedure worked well for the *m*- and *p*-hydroxy acetophenones, but not for the *o*-hydroxy substituted derivative. Analysis of the NMR spectra of the isolated compounds **122** and **123** indicated that these chalcones corresponded to the *Z*-isomers (Scheme 2), in contrast with the results obtained when using NaOH.

Given the lower reactivity of the free hydroxy substituted aldehydes in the aldolic condensation, the protection of the 2,4-hydroxy groups of **121** was necessary. For this purpose the MOM protecting group was chosen [27]. Condensation of the protected aldehyde **124** with either *o*-, *m*-, or *p*-hydroxyacetophenone and further treatment with HCl to remove the MOM group led to the formation of the expected compounds **125**–**127** (Scheme 3).

In the case of the *o*-hydroxy derivative **125**, flavanone **128** was also isolated after treatment with HCl. The formation of the flavanone isomer in acid medium is in agreement with the study performed by J. Mai et al. for chalcones *o*-hydroxy substituted in ring A [28].

Condensation of the 2,5-dimethoxyacetophenone **129** and the 4-acetylaminobenzaldehyde **130**, led to 4-acetylamino-chalcone **131** along with the 4-amino derivative **132**, resulting from the partial deacetylation of **131** during the coupling reaction. Removal of methoxy groups in **131** gave **133**, while treatment of **132** with BBr_3 (4 equiv) allowed the isolation of the fully deprotected compound **134** (Scheme 4). A partially deprotected chalcone was also detected in this latter reaction (HPLC-MS data).

Finally, substitution of ring B by an indol system was contemplated, both to study the effect of the replacement of one of the phenyl rings by a heterocyclic system, and also because of the activity shown by the 5-hydroxyindol as Type I PAM of α7 nAChR [29,30]. Condensation of 2,5-dimethoxyacetophenone **129** with 5-methoxyindol-3-carboxaldehyde **135** led to the formation of chalcone **136**, which upon demethylation gave the expected trihydroxy derivative **137** (Scheme 5).

All products were purified by flash or medium-pressure chromatography over silica gel or in reverse phase, as indicated in each case (Experimental section). Final compounds were

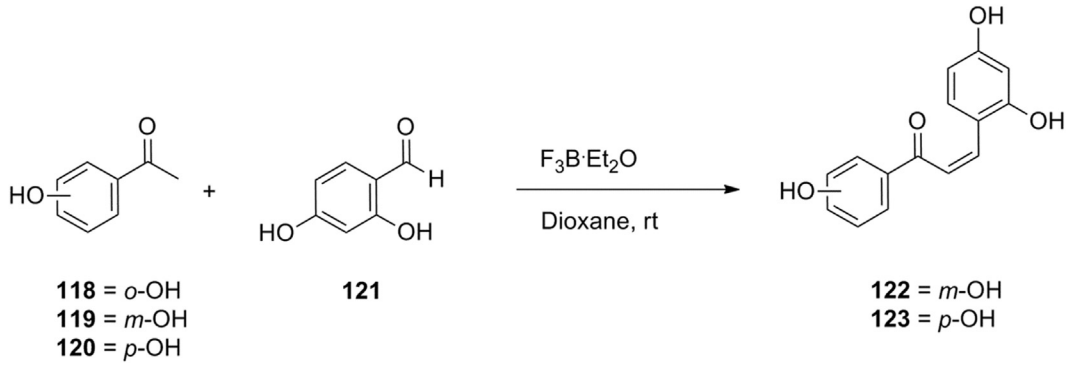

Scheme 2.

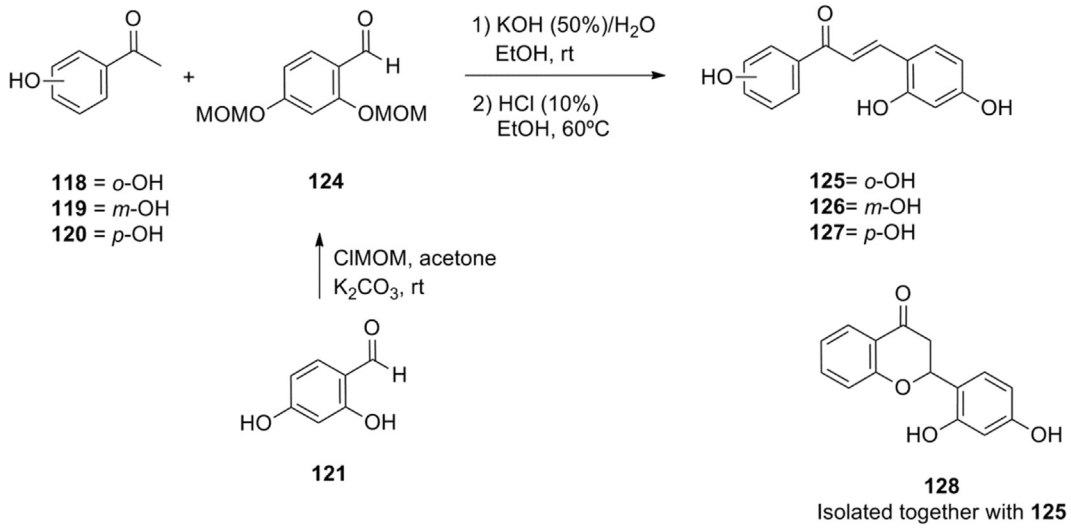

Scheme 3.

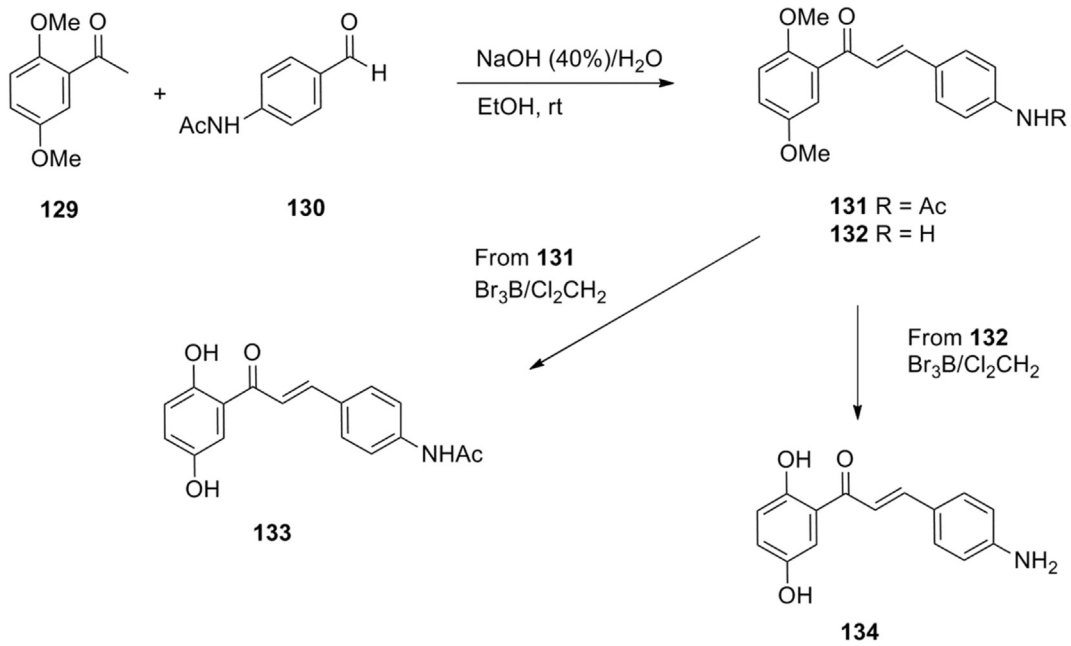

Scheme 4.

crystallized whenever possible. Detailed spectroscopic analysis (^{1}H NMR, ^{13}C NMR, MS) permitted the unambiguous characterization of the prepared compounds. Identification of the position of OH and OMe groups in partially deprotected compounds was accomplished on the basis of bidimensional NMR experiments (HSQC, HMBC).

While studying the solubility of compound **111** in PBS buffer/2.5% DMSO, the formation of a certain amount of the *Z*-isomer was observed (starting from a 100% *E*-isomer solution, the formation of up to 35% of *Z*-isomer was observed in 5 days, according to HPLC-data). This transformation was performed at preparative scale to isolate the *Z*-isomer (**138**) and check its behavior in front of the α7 nACh receptor. The photo-isomerization of chalcones has been previously reported [31], being pH dependent and its feasibility has also been correlated with the substituents in the aromatic rings [32].

2.4. Structure–activity relationship (SAR) analysis of polyhydroxy-substituted chalcones

Table 1 summarizes the study of compounds in which hydroxy groups were present at different positions of the chalcone structure. Information about a few compounds previously analyzed (see Table S1) has been integrated with the data corresponding to the new synthesized derivatives to facilitate the SAR discussion.

Considering the whole collection of compounds tested, it seems that the presence of at least one hydroxy group in each aromatic ring of the molecule is necessary, but not sufficient for behaving as α7 nAChR PAM. Thus, compounds totally unsubstituted at ring A, **8** and **55** (Table S1), as well as non substituted ring B analogues, **25**, **26**, and **96** (Table 1) were inactive. Compound **24**, lacking the 4′-OH group of **1**, was ineffective as PAM of α7 nAChRs. Similarly, other analogues having only one OH at each ring, like **22** and **23**, were

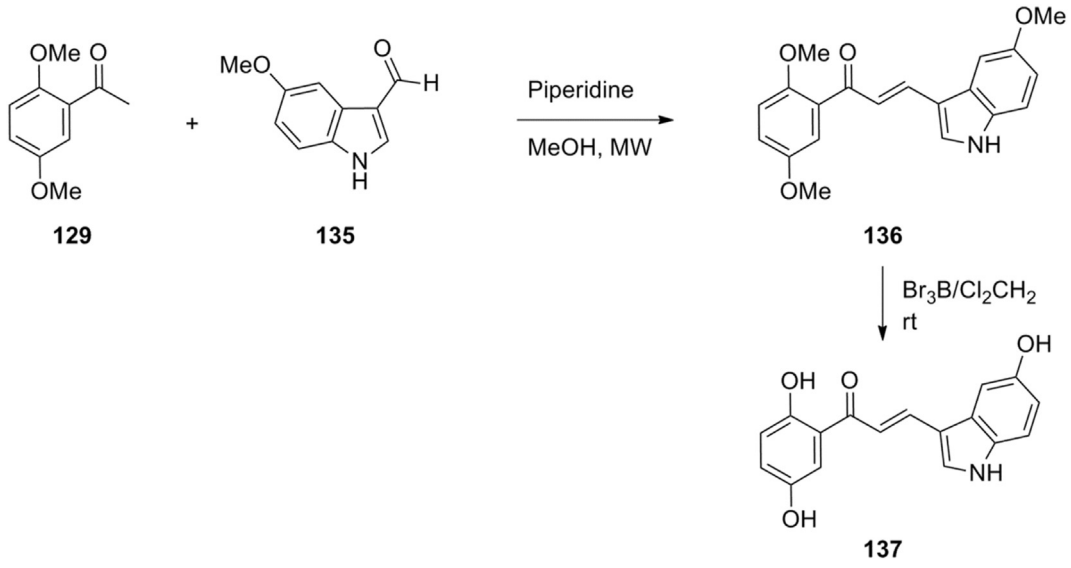

Scheme 5.

also inactive. By contrast, trihydroxylated compounds showed potentiating activity if, at least, one hydroxy group is present in each of the aromatic rings. As in **1**, the combination of monohydroxylated ring B, at either 2 or 4 position, and ring A 2′-4′- or 2′,5′-OHs, led to compounds with significant activity (Table 1, entries 6–9). In general, the 4-OH substitution is better than the 2-OH, and the 2′,5′-OH combination is preferred over the 2′,4′ one. In agreement with this, maximal activity was observed for the previously studied **97**, which has hydroxy groups at positions 4, 2′ and 5′. The double substitution at ring B (positions 2 and 4) combined with a single substitution at ring A (positions 2′, 3′ or 4′, compounds **125**, **126** and **127**, respectively) also produced compounds able to enhance currents with moderate/high effectiveness, although in a lesser extent than with **97**. For this reason, in the next step we explored tetrahydroxylated compounds. First, we decided to combine the substitutions of the best compounds **97** and **125**, namely two OHs at positions 2 and 4 of ring B with the ones present in ring A of **97** (2′ and 5′). This yielded compound **111**, which had the highest efficacy, close to **97**, but with higher potency. Requirements for hydroxy groups at the mentioned positions were evident when the tetrahydroxylated compound **117** was tested. Thus, the change of the OH from position 4 to 6 (ring B), keeping the rest as in **111**, resulted in an inactive compound. Merging one or two OHs in ring B and three hydroxyl groups in ring A (either at 2′,4′,5′ or 2′,4′,6′) resulted in tetra- and pentahydroxylated compounds (**100**, **101**, **115** and **116**) that reduced drastically or prevented both, effectiveness and potency. Curiously, the combination of 2,6-OH substituents in ring B resulted detrimental for activity, as deduced from the lack of potentiation observed with compounds **114** and **117**. All these data confirm that the convergence of four OH groups, preferentially at positions 2, 4, 2′ and 5′, constitutes the optimal substitution for activity.

Three *Z*-isomers, among them the **111** isomer, were also tested. Compound **123** (isomer of **127**) did not show any activity. Compound **122** behaved with moderate activity, like its *E*-isomer **126**. Finally, **138** was clearly less effective than its isomer **111**. Therefore, no gain is apparent with the *Z*-isomers.

Although most of the chalcones able to act as PAMs were polyhydroxylated, we detected four compounds with methoxy substituents having moderate potentiating activity. The three more effective ones (**87**, **112** and **113**) have in common the presence of OHs at positions 2′ and 5′ (like **111**) whereas methoxy groups are concentrated at different positions of ring B, suggesting that the latter can accommodate them without largely affecting PAM activity. Nevertheless, the presence of other substituents in this ring, such as the acetylamino and amino groups in position 4 of compounds **133** and **134**, respectively, abolished their PAM activity.

2.5. A comparison between compounds *97* and *111*

Fig. 4 features the main similarities and differences between compounds **97** and **111**, the most effective chalcones. When any of them was applied to oocytes expressing human α7 nAChRs, a large potentiating effect was observed in ACh-evoked ionic currents (Fig. 4c–d) but, unlike compound **1**, the currents decayed very slowly, so the changes in kinetics were similar to those found with type II PAMs. A detailed analysis of the kinetics of α7 nAChR currents induced by these and other chalcones is out of the scope of the present study. Nevertheless, the diversity of kinetic responses observed with different chalcones (for instance, **1** and **137** behave as type I whereas **97** and **111** are type II PAMs) might offer a unique opportunity to link both aspects, α7 kinetics and PAM structure (in preparation).

Both chalcones **97** and **111** showed similar concentration-dependent effectiveness (>30-fold potentiation at 200 μM of ACh, which is close to its EC_{50}), but **111** was about an order of magnitude more potent than **97**, as the potentiating EC_{50} were 3.3 μM and 25 μM for **111** and **97**, respectively (Fig. 4e–f). Potency of **111** is comparable to the one observed in similar conditions for other PAMs, such as PNU-120596 (EC_{50} 3.8–5.8 μM) [12,30], TQS (5.5 μM) [30] and A-867744 (1.1 μM) [33]. However, maximum efficacy is probably higher for **111** since we observed a 3400% maximal potentiation over the response with 0.2 mM ACh, whereas maximum efficacy values were only 541% for 5-hydroxyindol, 418% for TQS and 455% for PNU-1205964 when using 0.1 mM ACh [30].

The potentiating effect was not much dependent on ACh concentration. As shown in Fig. 4g–h, when 1 μM of each chalcone was co-applied with ACh the resulting ACh concentration–response relationships were only slightly shifted to the left, as the ACh EC_{50} values decreased from 176 μM (control) to 125 μM and 56 μM for **111** and **97**, respectively.

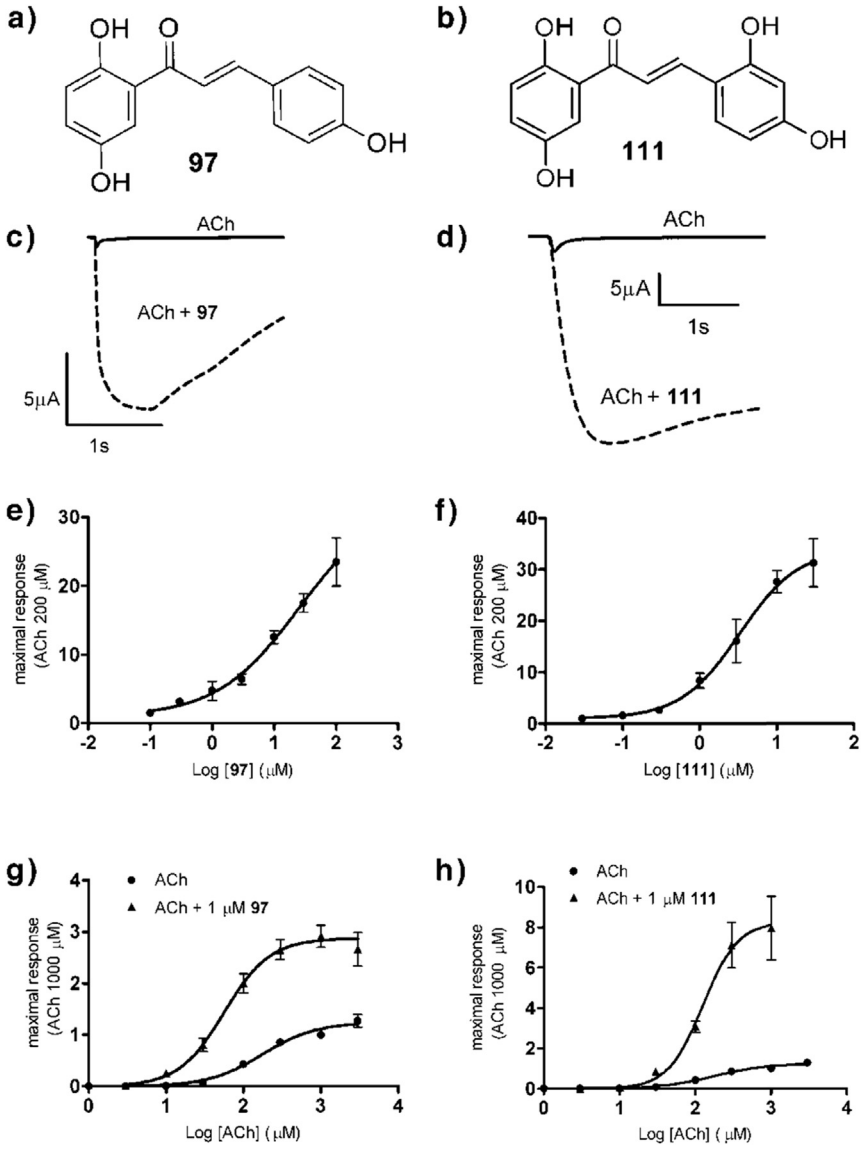

Fig. 4. Comparison between compounds **97** (left panels) and **111** (right panels). a–b) Chemical structure of chalcones **97** and **111**. c–d) Ionic currents recorded in representative oocytes expressing human α7 nAChRs. Currents were evoked by 600 ms applications of ACh 200 μM in the absence (continuous line) and in the presence (dotted line) of 30 μM of **97** or 3 μM of **111**. All currents were recorded at a holding potential of −80 mV. e–f) Concentration–response relationships for the potentiating effect of chalcones co-applied with ACh 200 μM. Continuous lines represent the fit to the Hill equation. Maximal potentiating effects were estimated as 33 and 34-fold, for **97** and **111**, respectively, with EC_{50} values of 25 μM and 3.3 μM for **97** and **111**, respectively. Notice that data for **97** are estimates since low solubility beyond 100 μM precluded the use of higher concentrations able to saturate the response. g–h) Acetylcholine concentration–response relationships in the absence (circles) and in the presence (triangles) of 1 μM of each chalcone. All data were normalized to the response obtained by ACh 1 mM in control conditions. Continuous lines represent fits to Hill equations, with estimated I_{max} and EC_{50} values of 1.3 and 176 μM (control), 2.9 and 56 μM (with **97**), and 8.3 and 125 μM (with **111**).

Consistent with their action as PAMs of α7 nAChRs, compounds **97** and **111** were unable to activate the later in the absence of ACh. Moreover, when tested for selectivity for α3β4 and α4β2 nAChR subtypes, they did not show activity as PAMs nor as agonists. Only a slight decline in the current evoked by ACh was observed (Table 2).

2.6. Toxicity studies of selected compounds (*97* and *111*)

The conjugated double bond in chalcones is a drug structural alert, since it can act as Michael acceptor toward nucleophiles. Moreover, chalcones display different biological activities, and can be considered within the so called privileged skeletons [34]. Because of this reactivity and promiscuity toward biological systems, before continuing the pharmacological exploration, some preliminary studies on the toxicity of the best compounds of the series were performed.

We first evaluated the cytotoxicity of **97** and **111** by performing the 3-(4,5-dimethylthiazol-2-yl)-2,5-diphenyl-2*H*-tetrazolium bromide (MTT) assay on HEK cells. The assay was made using a range of chalcone concentrations according to their EC_{50} values. Compound **97** (Fig. S1a) showed low toxicity even at high concentrations (up to 30 μM) whereas **111** (Fig. S1b) was completely non toxic at concentrations up to 10 μM. The lack of toxicity for this concentration was further validated in an alternative cell model, a primary culture of hippocampal postmitotic neurons (Fig. S2), delimitating a possible safe range of concentrations for compound **111** in future chronic exposures.

Table 2
Activity of **97** and **111** at Human α3β4 and α4β2 nAChRs Expressed in Xenopus Oocytes.[a]

Receptor	Compound	
	97	**111**
α3β4	87 ± 2.6 (5)[b]	93 ± 1.2 (3)[c]
α4β2	83 ± 4.9 (3)[d]	98 ± 1.8 (3)
α7	1258 ± 95 (7)[b]	2760 ± 220 (5)[b]

[a] Responses in the presence of 10 μM of the indicated compound and 50 μM ACh were recorded at −80 mV and normalized with respect to that shown by only ACh (100). For comparative purposes, α7 nAChRs were also tested in the same experiment with 200 μM ACh and the same concentration of compounds. Data are the mean ± SD, with *n* indicated in parentheses.
[b] $p < 0.001$.
[c] $p < 0.01$.
[d] $p < 0.05$.

To anticipate possible off-target adverse effects, which can occur by interaction of our chalcone derivatives with other unintended targets, we evaluated the effects of the most promising compounds on isolated organs and arterial blood pressure. Compounds **97** and **111** had no systemic effects on isolated organs of the rat such as atria (force or beating frequency), *vas deferens* (spontaneous and voltage-stimulated contraction), ileum (peristaltic force or frequency) and phrenic-diaphragm muscle preparation, at concentrations ranging from 0.01 to 100 μM (data not shown).

Compound **111** promoted a dose-dependent reduction in the heart rate, which was evident after the *i.v.* infusion of 1 μg/kg (Fig. S3) and a fall in the blood pressure although it was only significant at the higher dose tested (100 μg/kg). Given the lack of effect of this compound on isolated atria, its action *in vivo* probably reflects a central role or a stimulation of parasympathetic ganglia. Furthermore, given the antioxidant properties of some hydroxychalcones, including **1** [15], the blood pressure decline induced by **111** could also be related to a decrease in the oxidative stress, correlated itself to endothelial-dependent relaxation of blood vessels [35].

In general, a low toxicity profile was found for these compounds, encouraging further pharmacological studies.

2.7. Neuroprotection against cell death induced by rotenone and oligomycin-A (R/O)

It is well known that treatment with rotenone and oligomycin-A induces an oxidative impairment through the blockade of mitochondrial complexes I and V, respectively [36]. The potential cytoprotective effect of **111** on this cytotoxicity protocol was verified in HT22 cells, a hippocampal neuronal cell line having functional cholinergic properties [37] and expressing α7 nAChR subunits (Fig. S4). HT22 cells exposed for 24 h to R/O reduced their viability to 66% compared to control cells (100%), measured as MTT reduction (Fig. 5). Compound **111** preincubated for 24 h, and coincubated with 30 μM rotenone and 1 μM oligomycin-A for an additional 24 h-period, significantly increased viability of HT22 cells by 77 and 83% at 1 and 10 μM, respectively (Fig. 5). This effect appears to be mediated by α7 nAChRs since it was prevented by previous incubation with 0.1 μM α-Bgt, an almost irreversible antagonist. Moreover, at the same concentration than **111** (10 μM), the specific α7 nAChR agonist PNU-282987 showed a similar neuroprotective effect (84% viability), also prevented by α-Bgt. These results are in line with previous ones showing that α7 nAChR agonists such as PNU-282987 [38,39], SEN12333 [40] and DMXBA [41], as well as PAMs such as PNU-120596 [42] and isoliquiritigenin [19,20,43] display neuroprotective properties. Hence, our data indicate that **111** deserves further investigations as a neuroprotective compound.

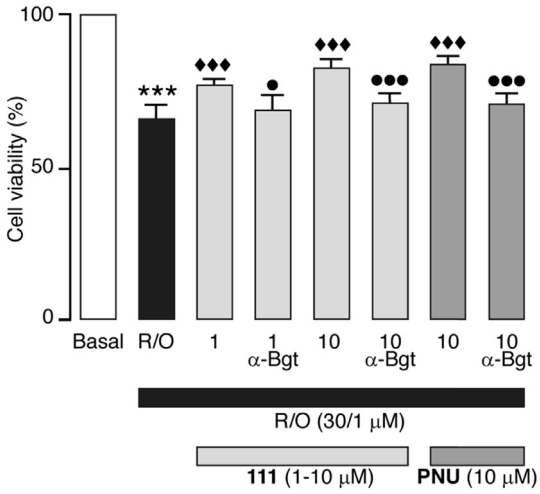

Fig. 5. Cytoprotection against cell death induced by 30 μM rotenone and 1 μM oligomycin-A. HT22 cells were preincubated either with 1 or 10 μM of compound **111** for 24 h, followed by R/O treatment for 24 h. Similar cultures were preincubated with 0.1 μM α-Bgt for 10 min before treatment with compound **111**. Each column represents the mean + S.E.M. of four different cell batches seeded in triplicate wells. A positive control was performed by incubating with 10 μM of the α7 agonist PNU-282987 in the same conditions that compound **111**. Pretreatment with 0.1 μM α-Bgt was also used in this case to prevent the effect of the agonist. Statistical analysis was performed by one-way ANOVA, followed by Newman–Keuls test. ***$P < 0.001$ as compared with the basal group; ♦♦♦$P < 0.001$ as compared with R/O group; • $P < 0.05$, ••• $P < 0.001$ as compared with the corresponding group without preincubation with α-Bgt.

2.8. Analgesic activity of *111* compared to a typical type II PAM

Since PAMs of α7 nAChRs, especially the type II PAM PNU-120596, are able to produce anti-nociceptive effects [44–46], we next addressed the question of whether the most potent chalcone, **111**, might reduce the thermal or mechanical hyperalgesia that results from inflammation induced by complete Freund's adjuvant (CFA). Intraplantar injection of CFA produces a significant inflammation that might last up to ≥20 days [47]. Thermal and mechanical hyperalgesia in the inflamed paw could be seen 24 h after CFA injection, as evidenced by the 2-fold reduction in the latency time response to a mildly noxious thermal or mechanical stimulus (Fig. 6).

We compared the effects of PNU-120596 and **111** in the CFA test. Lack of antinociceptive activity in the thermal hyperalgesia test was observed up to 4 h after the administration of both compounds (Fig. 6(a and b), respectively). In contrast, they almost abolished mechanical hyperalgesia at doses of 10 mg/kg (Fig. 6(c and d)). The analgesic effect was transient and disappeared completely 2 h after drug inoculation, probably because of pharmacokinetic drug clearance. Taken together, these results indicate that the level of analgesic activity exhibited by **111** was comparable to that exerted by PNU-120596. In spite of this parallelism, we cannot discard the possibility that **111** is also acting on other analgesic-related pathways. For instance, some chalcone derivatives like 2′,5′-dimethoxy-3,4-dihydroxychalcone have been reported as potent 5-lipoxygenase and cyclooxygenase inhibitors [48], whereas 2′,3-dihydroxy-, 2′,5′-dihydroxy-4-chloro-, and 2′,5′-dihydroxy-chalcones showed remarkable inhibitory effects on hind-paw edema induced by polymyxin B [49].

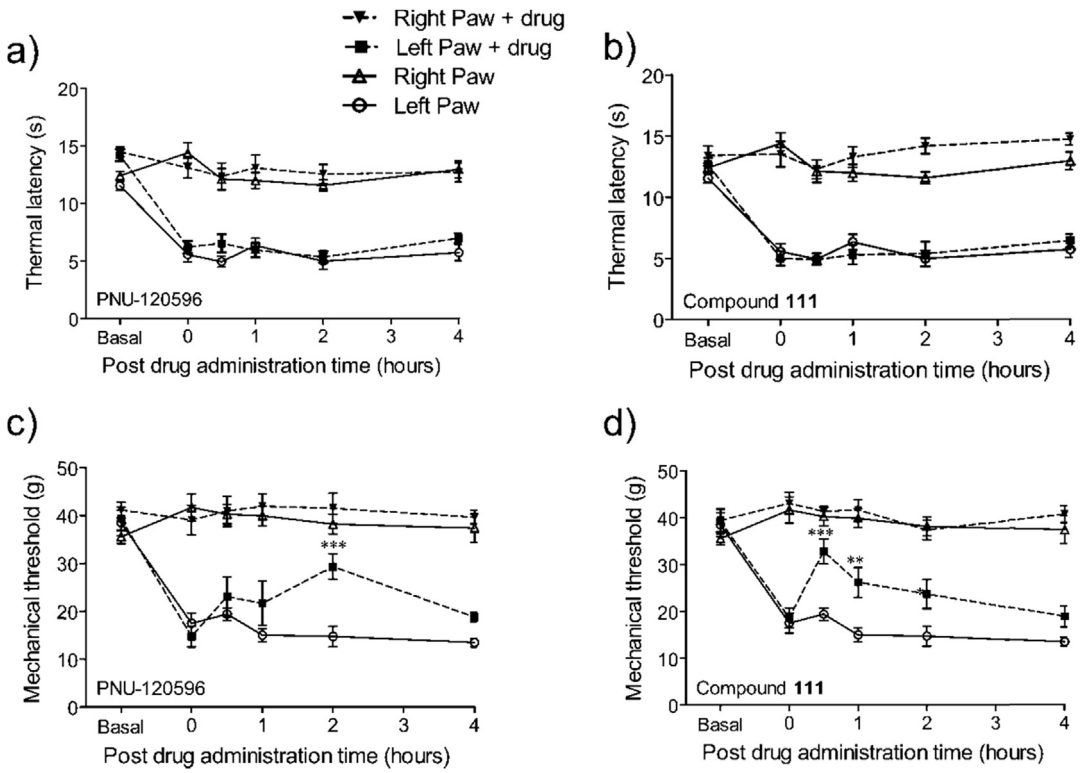

Fig. 6. Effects of PNU-120596 (left panels) and **111** (right panels), in the CFA-induced paw inflammation model. Time course of thermal (a,b) and mechanical (c,d) hyperalgesia in rats after injection of CFA 0.5 mg/mL (50 μL) into the left hind paw with and without administration of compound (10 mg/kg i.v.) The diagram shows the paw withdrawal latencies in response to thermal or mechanical stimulation ($n \geq 6$ rats/group). Data are given as mean ± SEM with $n = 6$. 2-way ANOVA with Bonferroni post hoc test. $^{*}P < 0.05$; $^{**}P < 0.01$, $^{***}P < 0.001$.

2.9. *Effect of compound **111** in learning ability*

Considering the cognitive effects observed upon α7 nAChR stimulation [5], we tested **111** on the water maze Morris' test. We chose old mice (14 months old) that were tested along 5 successive days; the results obtained the last day are summarized in Fig. 7. Each day, two hours before the test, animals received vehicle (control, C) or 1, 10 or 100 μg/kg compound **111**. An improvement in the learning performance was observed, being significant at the 10 μg/kg dose. In this case the time required to reach the hidden platform was reduced to half, suggesting a positive effect of **111** in cognitive functions as previously observed for other PAM [50].

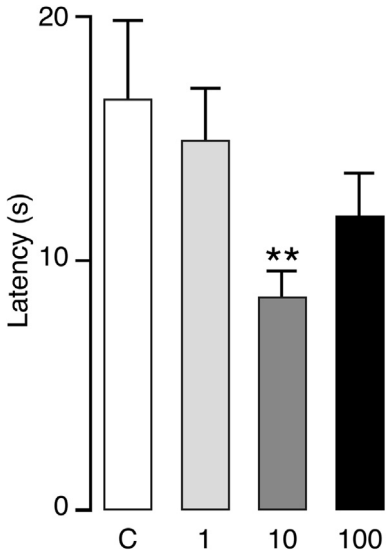

Fig. 7. Effect of compound **111** on the spatial memory. Morris water maze was used to test the effect of **111** on the ability of 14 months old mice to remember the situation of a hidden platform. The test was repeated daily during the 5 days of treatment with i.p. injections of vehicle (C) or the indicated doses of **111** administered one hour before the experiment ($n = 5$–16 mice). $^{**}p < 0.01$, Dunnet test.

3. Conclusions

A library of natural compounds was screened *in vitro* for PAMs of α7 nAChRs. A trihydroxy-substituted chalcone, isoliquiritigenin, showed moderate effectivity as PAM. Further screening of differently substituted chalcones allowed a detailed SAR analysis that oriented the synthesis of new compounds with improved efficacy and potency, especially compound **111**, a chalcone tetrahydroxylated at positions 2, 4, 2′ and 5′. The maximal potentiation was above 30-fold the current observed with only ACh, with an EC_{50} value of 3.3 μM. The macroscopic kinetics of α7 nAChR current was also modified in the presence of **111**, especially current decay time was much larger (i.e. **111** inhibited α7 receptor desensitization).

Compound **111** not only showed lack of cytotoxicity on HEK cells and primary hippocampal neurons but also no systemic effects on different isolated organs of the rat, except for a slight decline in blood pressure at high doses. Given the involvement of α7 nAChRs in pain and inflammation processes [7,8], compound **111** and future related derivatives should be considered useful therapeutic tools, as our analgesia experiments indicate. Moreover, chalcone **111** protected against the R/O-induced cell death of hippocampal neuronal HT22 cells, suggesting its potential as neuroprotective during increased oxidative stress.

Cognitive impairment is observed upon deficits in cholinergic neurotransmission driven, at least in part, by α7 nAChRs [4,5]. Presumably as a consequence of its potentiation of α7 nAChRs, compound **111** showed an improvement in cognitive performance when used in aged mice during the Morris' test. These results suggest the potential therapeutic utility of **111** in aging-related neurodegenerative conditions like Alzheimer's disease.

Because of the high efficacy in potentiating α7 nAChRs and the consequent promising effects as neuroprotective, analgesic and cognitive enhancer, we conclude that **111** and other chalcone derivatives represent a novel class of modulators with relatively simple structure to be used as departure point in future developments.

4. Experimental section

4.1. Chemistry

4.1.1. General

All reagents were of commercial quality. Solvents were dried and purified by standard methods. Analytical TLC was performed on aluminum sheets coated with a 0.2 mm layer of silica gel 60 F254. Silica gel 60 (230–400 mesh) was used for flash chromatography. Some compounds were purified by MPLC using SNAP 12g KP-C18-HS cartridges on an ISOLERA ONE (Biotage) apparatus. Mixtures of CH_3CN (solvent A), H_2O + 0.05% TFA (solvent B) were used as mobile phase. Unless indicated, all compounds were isolated in a purity ≥95% (HPLC data). Analytical HPLC-MS was performed on a Waters equipment coupled to a single quadrupole ESI-MS (Waters Micromass ZQ 2000) using a reverse-phase SunFire™ C18 4.6 × 50 mm column (3.5 μm) at a flow rate of 1 mL/min and by using a diodo array UV detector. Mixtures of CH_3CN + 0.08% formic acid (solvent A) and H_2O + 0.1% formic acid (solvent B) were used as mobile phase (gradient of 15–95% of A in B in 5 or 10 min, as indicated in each case). HRMS (EI+) was carried out in an Agilent 6520 Accurate-Mass Q-TOF LC/MS equipment. NMR spectra were recorded on a Varian-INOVA 300, a Bruker-AVANCE 300, a Varian-MERCURY 400, a Varian-INOVA 400 or a Varian System 500 spectrometer operating at 300, 400 or 500 MHz for ^1H and at 75, 100, and 125 MHz for ^{13}C recording. To confirm the NMR peak assignments, COSY and HSQC experiments were performed when necessary (For H and C numbering see Table 1 heading formula). Microwave assisted reactions were carried out in a Biotage Initiator Classic synthesizer. Melting points were determined on a Mettler MP70 apparatus and are uncorrected.

Compounds **1**–**101** were commercially available and purchased to Indofine, New Jersey, USA.

Structure of compounds **104**, **105**, **109**, **110**, **127**, **131** and **132** were confirmed by comparison of their physical data with those reported in the literature.

4.1.2. General procedure for the synthesis of methoxy-substituted chalcones

To a solution of the conveniently substituted benzaldehyde (1.91 mmol) in EtOH (15 mL), the desired acetophenone (1.66 mmol) was added. The solution was cooled at 0 °C, and an aqueous solution of NaOH 40% (1.87 mL) was slowly added. After 15 h of stirring at room temperature water was added and the organic solvent was removed at reduced pressure. The organic phase was extracted with EtAcO, and the organic extracts were washed with H_2O and brine. After drying with $MgSO_4$, the solvent was removed to dryness and the resulting residue crystallized from MeOH. Characterization data for all new methoxy-substituted chalcones can be found in the SI.

4.1.3. General procedure for the synthesis of polyhydroxylated chalcones

To a previously cooled solution (0 °C) of the corresponding methoxy substituted chalcone (0.609 mmol) in dried DCM (15 mL), a 1 M solution of BBr_3 in DCM (2 equiv for each MeO- group plus 2 more equiv for every group containing a potentially basic N or O) was slowly added under Ar atmosphere. After stirring 24–48 h at room temperature under Ar, H_2O was added to the reaction mixture. If a solid precipitate was formed, it was separated by filtration and washed with H_2O and DCM. When no precipitate was observed, the product was extracted with EtOAc. The organic extracts were washed with H_2O and brine, dried over Na_2SO_4 and then evaporated. The crude product was purified as indicated in each case.

*4.1.3.1. (E)-1-(2′,5′-Dihydroxyphenyl)-3-(2,4-dihydroxyphenyl)-2-propen-1-one (**111**).* Prepared from **104** using 10 equiv of Br_3B, which led also to the formation of **112**. Red solid (0.048 g, 29%) mp 180–182 °C. Purified twice by reverse-phase MPLC; gradient: 2 to 25 of CH_3CN in H_20 + 0.05% TFA. HPLC-MS: t_R = 3.89 min (5 min gradient). ^1H NMR (400 MHz, DMSO-d_6) δ: 6.33 (dd, 1H, J = 8.6, 2.3 Hz, 5-H), 6.40 (d, 1H, J = 2.3 Hz, 3-H), 6.81 (d, 1H, J = 8.8 Hz, 3′-H), 7.00 (dd, 1H, J = 8.8, 2.9 Hz, 4′-H), 7.41 (d, 1H, J = 2.9 Hz, 6′-H), 7.67 (d, 1H, J = 15.5 Hz, H_α), 7.67 (d, 1H, J = 8.6 Hz, 6-H), 8.04 (d, 1H, J = 15.5 Hz, H_β), 9.14, 10.07, 10.33 and 12.24 (s, 1H, OH). ^{13}C NMR (100 MHz, DMSO-d_6) δ:102.48 (C-3), 108.20 (C-5), 113.25 (C-6′), 114.44 (C), 116.26 (Cα), 118.28 (C-3′), 120.58 (C), 123.96 (C-4′), 131.29 (C-6), 141.37 (Cβ), 149.28 (C), 154.96 (C), 159.62 (C), 161.94 (C), 193.31 (CO) ppm. EM (ESI^+): m/z 273.5 $(M+H)^+$. HRMS (ESI^+) m/z calcd for $C_{15}H_{12}O_5$ $[M+1]^+$ 273.0757, found 273.0763.

*4.1.3.2. (E)-1-(2′,5′-Dihydroxyphenyl)-3-(2,4-dimethoxyphenyl)-2-propen-1-one (**112**).* Prepared from **104** using 5 equiv of Br_3B which led also to the formation of **111**. Red oil (0.45 g, 13%). Purified by column chromatography, eluent: CH_2Cl_2: MeOH, 30: 1. HPLC-MS: t_R = 9.23 min (10 min gradient). ^1H NMR (400 MHz, DMSO-d_6): δ 3.85 (s, 3H, OCH_3), 3.92 (s, 3H, OCH_3), 6.646.64 (m, 2H, 3-H and 5-H), 6.82 (d, 1H, J = 8.9 Hz, 3′-H), 7.01 (dd, 1H, J = 8.9, 2.8 Hz, 4′-H), 7.44 (d, 1H, J = 2.8 Hz, 6′-H), 7.76 (d, 1H, J = 15.6 Hz, H_α), 7.91 (d, 1H, J = 8.4 Hz, 6-H), 8.04 (d, 1H, J = 15.6 Hz, H_β), 9.16 and 12.08 (s, 1H, OH). ^{13}C NMR (100 MHz, DMSO-d_6) δ: 46.62 (OCH_3), 46.92 (OCH_3), 89.34 (C-3), 97.53 (C-5), 105.68 (C-6′), 106.75 (C-3′), 109,11 (C), 109.58 (C_α), 111.69 (C), 115.18 (C-4′), 121.85 (C-6), 130.66 (C_β), 140.39 (C), 145.88 (C), 151.28 (C), 154.48 (C), 184.22 (CO) ppm. EM (ESI^+): m/z 301.3 $(M+H)^+$. HRMS (ESI^+) m/z calcd for $C_{17}H_{16}O_5$ $[M+H]^+$ 301.1071, found 301.1081.

*4.1.3.3. (E)-1-(2′,5′-Dihydroxyphenyl)-3-(2-hydroxy-4,6-dimetoxyphenyl)-2-propen-1-one (**113**).* Prepared from **105** using 6 equiv of Br_3B, which led also to the formation of **114**. Red oil (0.019 g, 9%, 91% purity). Purification by MPLC in reverse-phase, eluent: gradient from 10 to 40% of A in B. HPLC-MS: t_R = 4.41 min (5 min gradient). ^1H NMR (400 MHz, DMSO-d_6) δ: 3.79 (s, 3H, OCH_3), 3.90 (s, 3H, OCH_3), 6.17 (s, 1H, 3-H), 6.18 (s, 1H, 5-H), 6.81 (d, 1H, J = 8.9 Hz, 3′-H), 6.99 (dd, 1H, J = 8.9, 2.9 Hz, 4′-H), 7.23 (d, 1H, J = 2.9 Hz, 6′-H), 7.93 (d, 1H, J = 15.6 Hz, H_α), 8.22 (d, 1H, J = 15.6 Hz, H_β), 9.24, 9.35 and 12.34 (s, 1H, OH). ^{13}C NMR (100 MHz, DMSO-d_6) δ: 55.35 (OCH_3), 56.03 (OCH_3), 90.43 (C-3), 93.77 (C-5), 104.47 (C), 113.65 (C-6′), 118.19 (C_α), 118.57 (C-3′), 120.43 (C), 124.04 (C-4′), 137.08 (C_β), 149.27 (C), 155.11 (C), 160.87 (C), 161.74 (C), 163.47 (C), 193.93 (CO) ppm. EM (ESI^+): m/z 317.4 $(M + H)^+$. HRMS (ESI^+) m/z calcd for $C_{17}H_{16}O_6$ $[M+H]^+$ 317.1020, found 317.1005.

*4.1.3.4. (E)-1-(2′,5′-Dihydroxyphenyl)-3-(2,6-dihydroxy-4-methoxyphenyl)-2-propen-1-one (**114**).* Prepared from **105** using

6 equiv of Br_3B, which led also to the formation of **113**. Red oil (0.049.g, 26%, 90% purity). Purified by reverse-phase MPLC. Gradient from 10 to 40% of CH_3CN in H_20 + 0.05% TFA. HPLC-MS: t_R = 3.83 min (5 min gradient) ^{1}H NMR (400 MHz, DMSO-d_6) δ: 3.71 (s, 3H, OCH_3), 6.03 (s, 2H, 3-H and 5-H) (These two protons are equivalent) 6.81 (d, 1H, J = 8.9 Hz, 3′-H), 6.98 (dd, 1H, J = 8.9, 2.8 Hz, 4′-H), 7.21 (d, 1H, J = 2.8 Hz, 6′-H), 7.95 (d, 1H, J = 15.5 Hz, H_α), 8.24 (d, 1H, J = 15.5 Hz, H_β), 12.43, 13.30, 13.42 and 13.69 (s, 1H, OH). ^{13}C NMR (100 MHz, DMSO-d_6) δ: 55.05 (OCH_3), 93.01 (C-3, C-5), 104.08 (C), 113.61 (C-6′), 117.63 (C_α), 118.53 (C-3′), 120.41 (C), 123.98 (C-4′), 138.11 (C_β), 149.23 (C), 155.16 (C), 160.78 (C), 163.13 (C), 194.01 (CO). EM (ESI$^+$): m/z 303.4 (M+H)$^+$. HRMS (ESI+) m/z calcd for $C_{16}H_{14}O_6$ [M+H]$^+$ 303.0863, found 303.0868.

*4.1.3.5. (E)-3-(2-Hydroxyphenyl)-1-(2′,4′,5′-trihydroxyphenyl)-2-propen-1-one (**115**).* Prepared from **106** using 10 equiv of Br_3B. Amorphous red solid (0.038 g, 23%) mp > 212 °C$^{(dec)}$. Purified by reverse-phase MPLC. Gradient: 10–30% CH_3CN in H_2O + 0.05% TFA. HPLC-MS: t_R = 5.36 min (10 min gradient). ^{1}H NMR (400 MHz, DMSO-d_6) δ: 6.32 (s, 1H, 6′-H), 6.87 (t, 1H, J = 7.4 Hz, 5-H), 6.94 (d, 1H, J = 8.2 Hz, 3-H), 7.27 (ddd, 1H, J = 8.2, 7.4, 1.5 Hz, 4-H), 7.45 (s, 1H, 3′-H), 7.80 (d, 1H, J = 15.7 Hz, H_α), 7.80 (dd, 1H, J = 1.5 Hz, 6-H), 8.06 (d, 1H, J = 15.6 Hz, H_β), 10.31 and 13.13 (s, 1H, OH) ppm. ^{13}C NMR (100 MHz, DMSO-d_6) δ: 103.11 (C-3′), 111.72 (C), 115.07 (C-6′), 116.26 (C-3), 119.48 (C-5), 120.36 (C), 121.41 (C_α), 129.30 (C-4), 132.00 (C-6), 138.40 (C_β), 139.02 (C), 154.99 (C), 157.30 (C), 159.34 (C), 191.36 (CO) ppm. EM (ESI$^+$): m/z 273.4 (M+H)$^+$. HRMS (ESI$^+$) m/z calcd for $C_{15}H_{12}O_5$ [M+H]$^+$ 273.0757, found 273.0752.

*4.1.3.6. (E)-3-(2,4-Dihydroxyphenyl)-1-(2′,4′,5′-trihydroxyphenyl)-2-propen-1-one (**116**).* Prepared from **107** using 10 equiv of Br_3B. Amorphous red solid (0.063 g, 36%) mp > 250 °C$^{(dec)}$. Purified by reverse-phase MPLC. Gradient: from 10 to 30 of CH_3CN in H_2O + 0.05% TFA. HPLC-MS: t_R = 4.42 min (10 min gradient). ^{1}H NMR (400 MHz, DMSO-d_6) δ: 6.29 (s, 1H, 6′-H), 6.32 (dd, 1H, J = 8.7, 2.3 Hz, 5-H), 6.39 (d, 1H, J = 2.3 Hz, 3-H), 7.42 (s, 1H, 3′-H), 7.58 (d, 1H, J = 15.5 Hz, H_α), 7.63 (d, 1H, J = 8.7 Hz, 6-H), 7.97 (d, 1H, J = 15.5 Hz, H_β), 8.71, 10.00, 10.26, 10.41 and 13.35 (s, 1H, OH) ppm. ^{13}C NMR (100 MHz, DMSO-d_6) δ: 102.51 (C-3′), 103.1 (C-3), 108.06 (C-5), 111.69 (C), 113.39 (C-6′), 114.86 (C), 116.16 (C_α), 131.08 (C-6), 138.19 (C_β), 139.89 (C), 154.48 (C), 159.16 (C), 159.27 (C), 161.48 (C), 191.36 (CO) ppm. EM (ES$^+$): 289.5 (M+H)$^+$. HRMS (ESI$^+$) m/z calcd for $C_{15}H_{12}O_6$ [M+H] $^+$ 289.0712, found 289.0704. EM (ESI$^+$): m/z 289.5 (M+H)$^+$. HRMS (ESI$^+$) m/z calcd for $C_{15}H_{12}O_6$ [M+H] $^+$ 289.0707, found 289.0704.

*4.1.3.7. (E)-1-(2′,5′-Dihydroxyphenyl)-3-(2,6-dihydroxyphenyl)-2-propen-1-one (**117**).* Prepared from **108** using 10 equiv of Br_3B. Amorphous red solid (0.062 g, 38%) mp > 250 °C$^{(dec)}$. Purified by reverse-phase MPLC. Gradient from 10 to 30 of CH_3CN in H_2O + 0.05% TFA; gradient: 10–30% of CH_3CN in H_2O + 0.05% TFA. HPLC-MS: t_R = 5.04 min (10 min gradient). ^{1}H NMR (400 MHz, DMSO-d_6) δ: 6.41 (d, 2H, J = 8.2 Hz, 3-H and 5-H), 6.83 (d, 1H, J = 8.9 Hz, 3′-H), 7.00 (dd, 1H, J = 8.9, 2.9 Hz, 4′-H), 7.06 (t, 1H, J = 8.2 Hz, 4-H), 7.22 (d, 1H, J = 2.9 Hz, 6′-H), 8.10 (d, 1H, J = 15.6 Hz, H_α), 8.26 (d, 1H, J = 15.6 Hz, H_β), 9.26, 10.36, 10.36 and 12.14 (s, 1H, OH) ppm. ^{13}C NMR (100 MHz, DMSO-d_6) δ: 106.65 (C-3, C-5), 109.73 (C), 113.80 (C-6′), 118.63 (C-3′), 120.60 (C-4′), 120.99 (C_α), 124.23 (C), 132.52 (C-4), 137.58 (C_β), 149.36 (C), 154.99 (C), 159.37 (C), 159.37 (C), 194.25 (CO) ppm. EM (ESI$^+$): m/z 273.3 (M + H)$^+$. HRMS (ESI$^+$) m/z calcd for $C_{15}H_{12}O_5$ [M+H]$^+$ 273.0757, found 273.0759.

*4.1.3.8. (E)-3-(2,4-Dihydroxyphenyl)-1-(2′-hydroxyphenyl)-2-propen-1-one (**125**).* Compound **128** was also isolated from the same reaction medium. Amorphous red solid (0.045 g, 12%), mp > 92 °C$^{(dec)}$. Purified by reverse-phase MPLC. Gradient from 2 to 50 of CH_3CN in H_2O + 0.05% TFA; gradient: 2–50% of CH_3CN in H_2O + 0.05% TFA. HPLC-MS: t_R = 8.47 min (10 min gradient). ^{1}H NMR (400 MHz, DMSO-d_6) δ: 6.30 (dd, 1H, J = 8.3, 2.3 Hz, 5-H), 6.36 (d, 1H, J = 2.3 Hz, 3-H), 6.97 (m, 2H, 4′-H and 6′-H), 7.50 (td, 1H, J = 8.3, 7.8, 1.6 Hz, 5′-H), 7.73 (d, 1H, J = 8.3 Hz, 6-H), 7.77 (d, 1H, J = 15.4 Hz, H_α), 8.13 (d, 1H, J = 15.4 Hz, H_β), 8.14 (dd, 1H, J = 7.3, 1.2 Hz, 3′-H), 10.07 (s, 1H, OH), 10.31 (s, 1H, OH), 12.98 (s, 1H, OH) ppm. ^{13}C NMR (100 MHz, DMSO-d_6) δ: 102.44 (C-3), 108.28 (C-5), 113.23 (C-3′), 115.69 (C-6′), 117.77 (C-4′), 119.03 (C-5′), 120.56 (C_α), 130.29 (C-6), 130.81 (C), 135.89 (C_β), 141.39 (C), 159.71 (C), 162.20 (C), 162.20 (C), 193.66 (CO) ppm. EM (ESI$^+$): m/z 257.3 (M+H)$^+$, 239.3 (M+H − H_2O). HRMS (ESI$^+$) m/z calcd for $C_{15}H_{12}O_4$ [M+H − H_2O]$^+$ 239.0703, found 239.0705.

*4.1.3.9. (E)-3-(2,4-Dihydroxyphenyl)-1-(3′-hydroxyphenyl)-2-propen-1-one (**126**).* Amorphous red solid (0.065 g, 18%), mp > 75 °C$^{(dec)}$. Purified by reverse-phase MPLC. Gradient from 2 to 50 of CH_3CN in H_20 + 0.05% TFA; gradient: 2–50% of CH_3CN in H_20 + 0.05% TFA. HPLC-MS: t_R = 6.62 min (10 min gradient). ^{1}H NMR (400 MHz, DMSO-d_6) δ: 6.31 (dd, 1H, J = 8.5, 2.1 Hz, 5-H), 6.38 (d, 1H, J = 2.1 Hz, 3-H), 6.97 (dd, 1H, J = 7.8, 1.2 Hz, 4′-H), 7.30 (t, 1H, J = 7.8 Hz, 5′-H), 7.34 (d, 1H, J = 1.2 Hz, 2′-H), 7.45 (dd, 1H, J = 7.8, 1.2 Hz, 6′-H), 7.56 (d, 1H, J = 15.6 Hz, H_α), 7.64 (d, 1H, J = 8.5 Hz, 6-H), 7.92 (d, 1H, J = 15.6 Hz, H_β), 9.77, 9.99 and 10.23 (s, 1H, OH) ppm. ^{13}C NMR (100 MHz, DMSO-d_6) δ: 102.50 (C-3), 108.03 (C-5), 113.34 (C), 114.41 (C-2′), 117.37 (C_α), 119.11 (C-6′), 119.64 (C-4′), 120.94 (C-5′), 129.76 (C-6), 130.61 (C), 140.21 (C_β), 157.65 (C), 159.20 (C), 161.44 (C), 189.23 (CO) ppm. EM (ESI$^+$): m/z 257.3 (M+H)$^+$, 239.3 (M+H − H_2O). HRMS (ESI$^+$) m/z calcd for $C_{15}H_{12}O_4$ [M+H]$^+$ 257.0808, found 257.0801.

*4.1.3.10. (E)-3-(2,4-Dihydroxyphenyl)-1-(4′-hydroxyphenyl)-2-propen-1-one (**127**).* Amorphous red solid (0.025 g, 20%), mp > 185 °C$^{(dec)}$ (lit.[48] 187–188 °C, 90% purity). Purified by reverse-phase MPLC. Gradient from 2 to 50 of CH_3CN in H_20 + 0.05% TFA; gradient: 2–50% of CH_3CN in H_20 + 0.05% TFA. HPLC-MS: t_R = 1.00 min (10 min gradient). ^{1}H NMR (400 MHz, DMSO-d_6) δ: 6.30 (dd, 1H, J = 8.7, 2.3 Hz, 5-H), 6.37 (d, 1H, J = 2.3 Hz, 3-H), 6.87 (d, 2H, J = 8.8 Hz, 2′-H, 6′-H), 7.61 (d, 1H, J = 15.9 Hz, H_α), 7.91 (d, 1H, J = 15.9 Hz, H_β), 7.95 (d, 1H, J = 8.7 Hz, 6-H), 7.96 (d, 2H, J = 8.8 Hz, 3′-H, 5′-H), 9.93, 10.15 and 10.33 (s, 1H, OH) ppm. ^{13}C NMR (100 MHz, DMSO-d_6) δ: 102.52 (C-3), 107.94 (C-5), 113.53 (C), 115.32 (C-5′, C-3′), 117.12 (C_α), 129.84 (C-6), 130.18 (C), 130.76 (C-2′, C-6′), 138.93 (C_β), 158.93 (C), 161.15 (C), 161.69 (C), 187.39 (CO) ppm. EM (ESI$^+$): m/z 239.3 (M+H − H_2O). HRMS (ESI$^+$) m/z calcd for $C_{15}H_{12}O_4$ [M+H − H_2O]$^+$ 239.0703, found 239.0701.

*4.1.3.11. (E)-3-(4-Acetylaminophenyl)-1-(2′,5′-dihydroxyphenyl)-2-propen-1-one (**133**).* Prepared from **131** using 8 equiv of Br_3B. Amorphous red solid (0.069 g, 38%, 92% purity) mp > 237 °C$^{(dec)}$. (HPLC-MS: t_R = 4.18 min (5 min gradient). ^{1}H NMR (400 MHz, DMSO- d_6) δ: 2.08 (s, 3H, OCH_3), 6.84 (d, 1H, J = 8.8 Hz, 3′-H), 7.04 (dd, 1H, J = 8.8, 2.9 Hz, 4′-H), 7.50 (d, 1H, J = 2.9 Hz, 6′-H), 7.68 (d, 2H, J = 8.6 Hz, 2-H and 6-H), 7.74 (d, 1H, J = 15.6 Hz, H_α), 7.80 (d, 1H, J = 15.6 Hz, H_β), 7.83 (d, 2H, J = 8.6 Hz, 3-H and 5-H), 10.20 (s, 1H, NH), 11.87 (s, 1H, OH). ^{13}C NMR (100 MHz, DMSO-d_6) δ: 24.16 (C–CH_3), 115.01 (C-6′), 118.27 (C-3′), 118.83 (C-2 and C-6), 120.07 (C_α), 120.89 (C), 124.27 (C-4′), 129.08 (C), 130.10 (C-3 and C-5), 141.84 (C), 144.35 (C_β), 149.45 (C), 154.66 (C), 168.70 (C–*CO*–NH), 193.11 (C–*CO*–C) ppm. EM (ESI$^+$): m/z 298.5 (M+H)$^+$. HRMS (ESI$^+$) m/z calcd for $C_{17}H_{15}NO_4$ [M+H]$^+$ 298.1074, found 298.1074.

*4.1.3.12. (E)-3-(4-Aminophenyl)-1-(2′,5′-dihydroxyphenyl)-2-propen-1-one (**134**).* Obtained from **132** (0.106 mmol) using 8 equiv

of Br_3B. Red solid (0.091 g, 58%, 93% purity) mp > 252 °C$^{(dec)}$. Purified by preparative centrifugally accelerated radial thin-layer chromatography (chromatotron), eluent: MeOH: CH_2Cl_2 (1:60) HPLC-MS: t_R = 4.22 min (5 min gradient). ^{1}H NMR (400 MHz, DMSO-d_6) δ: 6.03 (bs, 2H, NH_2), 6.60 (d, 2H, J = 8.3 Hz, 2-H and 6-H), 6.79 (d, 1H, J = 8.9 Hz, 3′-H), 7.00 (dd, 1H, J = 8.9, 2.7 Hz, 4′-H), 7.50 (d, 1H, J = 2.7 Hz, 6′-H), 7.56–7.60 (m, 3H, 3-H, 5-H and H_α), 7.72 (d, 1H, J = 14.8 Hz, H_β), 9.11 and 12.37 (s, 1H, OH) ppm. EM (ESI$^+$): *m/z* 256.4 (M+H)$^+$. HRMS (ESI$^+$) *m/z* calcd for $C_{15}H_{13}NO_3$ [M+H]$^+$ 256.0968, found 256.0964.

*4.1.3.13. (E)-1-(2′,5′-dihydroxyphenyl)-3-(5-hydroxy-1H-indol-3-yl)-2-propen-1-one (**137**).* Prepared from **136** using 10 equiv of Br_3B following the general procedure described above for polyhydroxy chalcones. Amorphous red solid (0.180 g, 80%). mp > 240 °C$^{(dec)}$. (HPLC-MS: t_R = 5.45 min (10 min gradient). ^{1}H NMR (400 MHz, DMSO-d_6) δ: 6.77 (dd, 1H, J = 8.7, 2.5 Hz, 6-H), 6.82 (d, 1H, J = 8.7 Hz, 7-H), 7.00 (dd, 1H, J = 8.7, 2.9 Hz, 4′-H), 7.31 (d, 1H, J = 8.7 Hz, 3′-H), 7.31, (d, 1H, J = 2.5 Hz, 4′-H), 7.41 (d, 1H, J = 2.9 Hz, 6′-H), 7.45 (d, 1H, J = 15.2 Hz, H_α), 8.06 (d, 1H, J = 3.0 Hz, 2-H), 8.10 (d, 1H, J = 15.2 Hz, H_β), 11.35 (d, 1H, J = 3.0 Hz, NH) ppm. ^{13}C NMR (100 MHz, DMSO-d_6) δ: 104.74 (C-4), 112.45 (C), 112.73 (C-3′), 112.84 (C-6′), 113.18 (C-6), 113.97 (C_α), 118.38 (C-7), 120.55 (C), 123.66 (C-4′), 126.06 (C), 131.80 (C), 134.85 (C-2), 140.70 (C_β), 149.26 (C), 152.88 (C), 154.98 (C), 192.48 (CO) ppm. EM (ESI$^+$): *m/z* 296.4 (M+H)$^+$. HRMS (ESI$^+$) *m/z* calcd for $C_{17}H_{13}NO_4$ [M+H]$^+$ 296.0917, found 296.0927.

*4.1.4. Preparation of polyhydroxy Z-chalcones **122** and **123***

To a solution of 2,4-dihydroxybenzaldehyde (0.4 g, 2.93 mmol) and the corresponding hydroxyacetophenone (0.2 g, 1.468 mmol) in 1,4-dioxane (12 mL), $BF_3.Et_2O$ (0.91 mL, 7.34 mmol) was added. The reaction mixture was stirred at room temperature for 24 h. After that, the precipitated solid was filtered and washed with methylene chloride leading to **122**, or **123** according to the hydroxyacetophenone used as starting material.

*4.1.4.1. (Z)-3-(2,4-Dihydroxyphenyl)-1-(3′-hydroxyphenyl)-2-propen-1-one (**122**).* Amorphous red solid (0.3 g, 80%, 92% purity), mp > 167 °C$^{(dec)}$. (HPLC-MS: t_R = 2.09 min (5 min gradient). ^{1}H NMR (500 MHz, DMSO-d_6) δ: 7.26 (ddd, 1H, J = 8.1, 2.2, 0.9 Hz, 4′-H), 7.49 (dd, 1H, J = 9.0, 2.2 Hz, 5-H), 7.52–7.59 (m, 2H, 3-H, 6′-H), 7.82 (t, 1H, J = 2.2 Hz, 2′-H), 7.96 (dd, 1H, J = 8.1, 0.9 Hz, 5′-H), 8.29 (d, 1H, J = 9.0 Hz, 6-H), 8.57 (d, 1H, J = 8.5 Hz, H_α), 9.37 (d, 1H, J = 8.5 Hz, H_β), 10.28 (brs, 2H, OH) ppm. ^{13}C NMR (125 MHz, DMSO-d_6) δ: 102.60 (C-3), 112.70 (C), 113.32 (C_α), 115.00 (C-2′), 119.06 (C), 120.16 (C-5), 120.33 (C-5′), 122.70 (C-4′), 123.01 (C-6′), 133.30 (C-6), 154.90 (C_β), 158.49 (C), 159.49 (C), 161.49 (C), 189.20 (CO) ppm. EM (ESI$^+$): *m/z* 239.3 (M+H − H_2O). HRMS (ESI$^+$) *m/z* calcd for $C_{15}H_{12}O_4$ [M+H − H_2O]$^+$ 239.0703, found 239.0698.

*4.1.4.2. (Z)-3-(2,4-Dihydroxyphenyl)-1-(4′-hydroxyphenyl)-2-propen-1-one (**123**).* Amorphous red solid (0.188 g, 50%), mp > 188 °C$^{(dec)}$. (HPLC-MS: t_R = 1.20 min (5 min gradient). ^{1}H NMR (400 MHz, DMSO-d_6) δ: 7.11 (d, 2H, J = 9.0 Hz, 2′-H and 6′-H), 7.40 (dd, 1H, J = 8.9, 2.2 Hz, 5-H), 7.51 (d, 1H, J = 2.2 Hz, 3-H), 8.18 (d, 1H, J = 8.9 Hz, 6-H), 8.41 (d, 1H, J = 8.7 Hz, H_α), 8.45 (d, 2H, J = 9.0 Hz, 3′-H, 5′-H), 9.19 (d, 1H, J = 8.7 Hz, H_β) ppm. ^{13}CNMR (100 MHz, DMSO-d_6) δ: 102.52 (C-3), 112.36 (C), 113.51 (C_α), 117.28 (C-3′, C-5′), 119.59 (C), 120.96 (C-5), 130.42 (C-6), 132.60 (C-2′ and C-6′), 153.18 (C_β), 158.68 (C), 161.43 (C), 165.96 (C), 187.41 (CO) ppm. EM (ESI$^+$): *m/z* 239.3 (M+H − H_2O). HRMS (ESI$^+$) *m/z* calcd for $C_{15}H_{12}O_4$ + H−H_2O]$^+$ 239.0703, found 239.0705.

*4.1.4.3. (Z)-1-(2′,5′-Dihydroxyphenyl)-3-(2,4-dihydroxyphenyl)-2-propen-1-one (**138**).* Prepared from **111** (20 mg) using 40 mL of PBS (with 2.5% DMSO). After five days the formation of a 35% of *Z* isomer was detected by HPLC-MS (an explanation has been included in the discussion section). The product was lyophilized and the inorganic salts were filtered off. The crude product was purified by reverse-phase MPLC (three times). Amorphous red solid (5 mg, 20%, 85% purity, no isomer *E* was detected at the sample). Gradient from 2 to 25 of CH_3CN in H_2O + 0.05% TFA; gradient: 2–25% of CH_3CN in H_2O + 0.05% TFA. HPLC-MS: t_R = 3.13 min (5 min gradient). ^{1}H NMR (400 MHz, DMSO-d_6) δ: 6.26 (dd, 1H, J = 8.4, 2.4 Hz, 5-H), 6.33 (d, 1H, J = 2.4 Hz, 3-H), 6.80 (d, 1H, J = 8.8 Hz, H_α), 6.90 (d, 1H, J = 8.8 Hz, H_β), 6.99 (dd, 1H, J = 8.4, 3.2 Hz, 4′-H), 7.11 (d, 1H, J = 8.9 Hz, 3′-H), 7.18 (d, 1H, J = 3.1 Hz, 6′-H), 7.22 (d, 1H, J = 8.4 Hz, 6-H), 9.23, 9.41, 9.63 and 11.33 (brs, 1H, OH). EM (ESI$^+$): *m/z* 273.5 (M+H)$^+$. HRMS (ESI$^+$) *m/z* calcd for $C_{15}H_{12}O_5$ + H]$^+$ 273.0757, found 273.0759.

4.2. Pharmacology

4.2.1. Oocyte expression and electrophysiological studies

All human nAChR cDNAs were cloned in derivatives of the pSP64T vector containing part of the pBluescript polylinker. Capped mRNA was synthesized *in vitro* using SP6 RNA polymerase, the mMESSAGE-mMACHINE kit from Ambion (Thermo Fisher Scientific, Madrid, Spain) and the pSP64T derivatives mentioned above. Defoliculated *X. laevis* oocytes were injected with 5 ng of each subunit cRNA in 50 nL of sterile water. All experiments were performed within 2–3 days after cRNA injection [51].

Unless otherwise specified, chalcones were pre-applied in the bath for 2 min and then co-applied with ACh through a pipette held very close to the oocyte for fast application.

Functional expression of each receptor was estimated as the peak ionic current evoked by 0.6 s application of 0.2 mM ACh at −80 mV. All experiments were performed at 22 °C. Current records were measured with Clampfit 10.0 (MDS Analytical Technologies, Sunnyvale, CA, USA).

Normalized peak currents were obtained by dividing the maximum value of the current obtained in the presence of chalcone by the maximum value of the current obtained in control conditions. Dose–response curves for the peak current obtained with ACh were fitted to the Hill equation: Normalized current = I_{max}/(1 + (EC_{50}/[ACh])^{nH}). Data are expressed as mean ± SEM.

4.2.2. Bovine chromaffin cells amperometry

Bovine chromaffin cells were isolated by adrenal medulla digestion with collagenase IA and further Urografin® centrifugation, as described [52]. Cells were suspended in a 1:1 mixture of Dulbecco's modified Eagle's (DMEM) and HAM's-F12 media supplemented with 5% fetal calf serum, 50 IU/mL penicillin and 50 μg/mL gentamicin and incubated at 37 °C/5% CO_2 and plated on 12-mm diameter glass coverslips at 5 × 10^4 cells density. Cells were used at room temperature between 1 and 3 days of culture. Carbon fiber microelectrodes of 5 μm radius (Thornel P-55; Amoco Corp., Greenville SC), were prepared as described [53]. Electrodes were calibrated in a flow cell and accepted for cell studies when the application of noradrenaline (50 μM) resulted in an oxidation current of 300–400 pA, which is reduced by 80–100 pA under stop-flow conditions. Amperometric measurements were performed with the carbon fiber microelectrode gently touching the cell membrane. Signals were low-pass filtered at 1 kHz and collected at 4 kHz using locally written software (LabView for Macintosh, National Instruments, Austin, TX, USA). Data analysis was conducted using locally written macros for IGOR (Wavemetrics, Lake Oswego, OR) [54].

4.2.3. Cytotoxicity assay

Cell viability was assessed by the detection of mitochondrial activity in living cells using a modified colorimetric analysis of Blue Tetrazolium Bromide Thiazolyl (MTT) [55,56]. Briefly, HEK293 cells (2×10^4 cells/well) were subcultured in 96-well plates, grown until 80–90% confluence, and incubated with increasing concentrations of chalcones for 24 h. Following treatment, 10 μL of MTT solution (5 mg/mL in phosphate buffered saline) was added to each well and further incubated for 4 h at 37 °C. Subsequently, 100 μL of DMSO was added to each well to dissolve any deposited formazan resulting from cleavage and reduction of MTT by active mitochondrial dehydrogenases [55]. The optical density of each well was measured at 540 nm with a microplate reader (Polastar BMG LABTECH, Offenberg, Germany).

Primary hippocampal neurons were seeded in 24-well plates at a density of 13×10^4 cells/well (see supporting information for detailed culture procedures). The day of plating was considered day *in vitro* 1 (1DIV). Neurons were incubated with compound **111** at 9DIV and measurements for cell viability and death were conducted 24 h later (10DIV) in three independent cultures. Cell viability was estimated using the MTT assay previously described for HEK293 cells whereas cell death was estimated using the lactate dehydrogenase assay (Cytotoxicity Detection kit PLUS (LDH), Roche Applied Science), according to manufacturer's instructions. As positive controls (100% of cytotoxicity), 2–3 wells per culture were treated with 1% Triton X-100, whose percentage of LDH activity in the medium related to basal (DMSO) was 387.4 ± 29.4%.

4.2.4. Culture and viability assay of hippocampal neuronal HT22 cells

HT22 cells were cultured in DMEM, supplemented with 10% heat-inactivated fetal bovine serum, 100 units/mL penicillin, and 100 μg/mL streptomycin. Cultures were seeded into flasks containing supplemented medium and kept at 37 °C in a humidified atmosphere of 5% CO_2 and 95% air. For assays, HT22 cells were subcultured in 48-well plates at a seeding density of 1×10^5 cells per well. Cells were treated with compound **111** before confluence in DMEM with 10% fetal bovine serum. Cells were used at a passage below 13.

Cell viability of HT22 cells was assessed by the MTT assay [55,56]. Briefly, 50 μL of the MTT labeling reagent, at a final concentration of 0.5 mg/mL, was added to the DMEM of each well at the end of the treatments period and the plate was placed in a humidified incubator at 37 °C with 5% CO_2 and 95% air (v/v) for an additional 2 h period. The resulting formazan was spectrophotometrically assayed as above. Results were compared to control samples, treated with vehicle (DMEM), to which 100% viability was attributed.

4.2.5. Analgesic activity

Male Wistar rats (250–300 g) were obtained from Janvier, France. All experiments were approved by the Institutional Animal and Ethical Committee of the Universidad Miguel Hernandez where experiments were conducted and they were in accordance with the guidelines of the Economic European Community and the Committee for Research and Ethical Issues of the International Association for the Study of Pain. All parts of the study concerning animal care were performed under the control of veterinarians.

CFA emulsion (1:1 oil/saline, 0.5 mg/mL) was injected into the plantar surface (50 μL) of the left hind paw of rats [57]. Compounds were administered at 10 mg/kg i.v. 24 h after CFA injection. Thermal hyperalgesia was monitored 24 h after CFA injection and up to 4 h after administering the compounds with an Ugo Basile Plantar Test (Hargreaves Apparatus). In brief, rats were habituated to an apparatus consisting of individual Perspex boxes on an elevated glass table. A mobile radiant heat source was located under the table and focused on the hind paw. Paw withdrawal latencies were defined as the time taken by the rat to remove its hind paw from the heat source. A cutoff point of 25 s was set to prevent tissue damage.

The mechanical allodynia was monitored 24 h after CFA injection and up to 4 h after administering the compounds. Paw withdrawal latency to mechanical stimulation was assessed with an automated testing device consisting of a steel rod that is pushed against the plantar surface of the paw with increasing force until the paw is withdrawn (Dynamic Plantar Aesthesiometer; Ugo Basile). The maximum force was set at 50 g to prevent tissue damage and the ramp speed was 2.5 g/s. Rats were placed in test cages with a metal grid bottom. They were kept in the test cages for 30–40 min to allow accommodation. The paw withdrawal latency was obtained as the mean of 3 consecutive assessments at each time point (at least 10 s between repeated measurements of the same paw).

4.2.6. Morris water maze test [58]

A plastic circular pool of 90 cm diameter was filled with reconstituted powdered milk to keep the surface opaque. For testing purposes, the pool was divided in eight equidistant entry points (N, NE, E, SE, S, SW, W, NW) along the whole circumference and a 10 cm diameter transparent circular disc placed one centimeter below the surface close to the SW point. The milky water was kept at 27 ± 1 °C and changed every other day. Several visual cues were positioned around the pool to facilitate the orientation of mice. Every animal performed 4 consecutive trials for 5 consecutive days, each trial as follows: with the experimenter standing immobile and silent on the same spot, the mouse was deposited in the pool face to the pool wall and left to swim until it reached the hidden escape disc or last swimming for 60 s (after which the mouse was placed on the disc), whatever happened first. The subject was allowed to rest on the disc for 30 s before being immersed again. After a 4 trials session, each one starting at a different place of the pool, the animal was cleaned and dried with a paper towel and a soft infrared light and returned to its cage. Each trial was recorded and analysis was performed using our dedicated software [59]. For analytical purposes, a mouse is considered as having reached the disc if it climbed completely or partially onto it and stood there for at least 2 s. Any mouse which was unable to swim or sunk frequently was removed from the experiment and its previous results discarded.

Transparency declarations

The authors declare no conflict of interest.

Acknowledgments

We thank Sara González-Reyes for her assistance in the synthesis of two starting compounds and Susana Gerber for technical assistance. This work was supported by grants from Spanish Ministry of Science and Innovation (currently Ministry of Economy and Competitivity): The Spanish Ion Channel Initiative-CONSOLIDER INGENIO 2010 (CSD2008-00005), SAF2009-09323, BFU2008-02160, SAF2011-22506, SAF2011-22802, SAF2012-23332, BFU2010-15822 and BFU2012-39092-C02-02. B.B. thanks the CSIC for a predoctoral fellowship (JAE-Predoc from Junta para la Ampliación de Estudios, co-financed by FSE). The Instituto de Neurociencias is a "Centre of Excellence Severo Ochoa".

Appendix A. Supplementary data

Supplementary data related to this article can be found at http://dx.doi.org/10.1016/j.ejmech.2014.09.039.

References

[1] R.L. Papke, Merging old and new perspectives on nicotinic acetylcholine receptors, Biochem. Pharmacol. 89 (2014) 1–11.
[2] E.X. Albuquerque, E.F.R. Pereira, M. Alkondon, S.W. Rogers, Mammalian nicotinic acetylcholine receptors: from structure to function, Physiol. Rev. 89 (2009) 73–120.
[3] D.K. Berg, W.G. Conroy, Nicotinic α7 receptors: synaptic options and downstream signaling in neurons, J. Neurobiol. 53 (2002) 512–523.
[4] H.R. Parri, C.M. Hernandez, K.T. Dineley, Research update: alpha7 nicotinic acetylcholine receptor mechanisms in Alzheimer's disease, Biochem. Pharmacol. 82 (2011) 931–942.
[5] B. Lendvai, F. Kassai, A. Szájli, Z. Némethy, α7 Nicotinic acetylcholine receptors and their role in cognition, Brain Res. Bull. 93 (2013) 86–96.
[6] J.W. Young, M.A. Geyer, Evaluating the role of the alpha-7 nicotinic acetylcholine receptor in the pathophysiology and treatment of schizophrenia, Biochem. Pharmacol. 86 (2013) 1122–1132.
[7] I.C. Umana, C.A. Daniele, D.S. McGehee, Neuronal nicotinic receptors as analgesic targets: It's a winding road, Biochem. Pharmacol. 86 (2013) 1208–1214.
[8] G. Matteoli, G.E. Boeckxstaens, The vagal innervation of the gut and immune homeostasis, Gut 62 (2013) 1214–1222.
[9] J.L. Galzi, S. Bertrand, P.-J. Corringer, J.-P. Changeux, D. Bertrand, Identification of calcium binding sites that regulate potentiation of a neuronal nicotinic acetylcholine receptor, EMBO J. 15 (1996) 5824–5832.
[10] V.V. Uteshev, The therapeutic promise of positive allosteric modulation of nicotinic receptors, Eur. J. Pharmacol. 727 (2014) 181–185.
[11] F. Chimienti, R.C. Hogg, L. Plantard, C. Lehmann, N. Brakch, J. Fischer, M. Huber, D. Bertrand, D. Hohl, Identification of SLURP-1 as an epidermal neuromodulator explains the clinical phenotype of Mal de Meleda, Hum. Mol. Genet. 12 (2003) 3017–3024.
[12] R.S. Hurst, M. Hajós, M. Raggenbass, T.M. Wall, N.R. Higdon, J.A. Lawson, K.L. Rutherford-Root, M.B. Berkenpas, W.E. Hoffmann, D.W. Piotrowski, V.E. Groppi, G. Allaman, R. Ogier, S. Bertrand, D. Bertrand, S.P. Arneric, A novel positive allosteric modulator of the α7 neuronal nicotinic acetylcholine receptor: *in vitro* and *in vivo* characterization, J. Neurosci. 25 (2005) 4396–4405.
[13] D.K. Williams, J. Wang, R.L. Papke, Positive allosteric modulators as an approach to nicotinic acetylcholine receptor-targeted therapeutics: advantages and limitations, Biochem. Pharmacol. 82 (2011) 915–930.
[14] S. Kumar, A. Sharma, B. Madan, V. Singhal, B. Ghosg, Isoliquiritigenin inhibits IκB kinase activity and ROS generation to block TNF-α induced expression of cell adhesion molecules on human endothelial cells, Biochem. Pharmacol. 73 (2007) 1602–1612.
[15] J. Vaya, P.A. Belinky, M. Aviram, Antioxidant constituents from licorice roots: isolation, structure elucidation and antioxidative capacity toward LDL oxidation, Free Radic. Biol. Med. 23 (1997) 302–313.
[16] H. Kakegawa, H. Matsumoto, T. Satoh, Inhibitory effects of some natural products on the activation of hyaluronidase and their anti-allergic actions, Chem. Pharm. Bull. 40 (1992) 1439–1442.
[17] S. Yamazaki, T. Morita, H. Endo, T. Hamamoto, M. Baba, Y. Joichi, S. Kaneko, Y. Okada, T. Okuyama, H. Nishini, A. Tokue, Isoliquiritigenin suppresses pulmonary metastasis of mouse renal cell carcinoma, Cancer Lett. 183 (2002) 23–30.
[18] T. Takahashi, N. Takasuka, M. Iigo, M. Baba, H. Nishino, H. Tsuda, T. Okuyama, Isoliquiritigenin, a flavonoid from licorice, reduces prostaglandin E2 and nitric oxide, causes apoptosis, and suppresses aberrant crypt foci development, Cancer Sci. 95 (2004) 448–453.
[19] C. Zhan, J. Yang, Protective effects of isoliquiritigenin in transient middle cerebral artery occlusion-induced focal cerebral ischemia in rats, Pharmacol. Res. 53 (2006) 303–309.
[20] M.J. Lee, C.H. Yang, J.-P. Jeon, M. Hwang, Protective effects of isoliquiritigenin against methamphetamine-induced neurotoxicity in mice, J. Pharmacol. Sci. 111 (2009) 216–220.
[21] A. Campos-Caro, F.I. Smillie, E. Domínguez del Toro, J.C. Rovira, F. Vicente-Agulló, J. Chapuli, J.M. Juíz, S. Sala, F. Sala, J.J. Ballesta, M. Criado, Neuronal nicotinic acetylcholine receptors on bovine chromaffin cells: cloning expression and genomic organization of receptor subunits, J. Neurochem. 68 (1997) 488–497.
[22] S. Khatib, O. Nerya, R. Musa, M. Shmuel, S. Tamir, J. Vaya, Chalcones as potent tyrosinase inhibitors: the importance of a 2,4-substituted resorcinol moiety, Bioorg. Med. Chem. 13 (2005) 433–441.
[23] J.F.W. McOmie, M.L. Watts, D.E. West, Demethylation of aryl methyl ethers by boron tribromide, Tetrahedron 24 (1968) 2289–2292.
[24] C. Chiruta, D. Schubert, R. Dargusch, P. Maher, Chemical modification of the multitarget neuroprotective compound Fisetin, J. Med. Chem. 55 (2012) 378–389.
[25] D. Huang, J.-X. Wang, Y. Hu, Y. Zhang, J. Tang, A new solvent-free synthesis of α,β-unsaturated ketones from acetals with aryl ketones under microwave irradiation, Synth. Commun. 32 (2002) 971–979.
[26] T. Narender, K. Papi Reddy, A simple and highly efficient method for the synthesis of chalcones by using borontrifluoride-etherate, Tet. Lett. 48 (2007) 3177–3180.
[27] B.-T. Kim, K.-J. O, J.-C. Chun, K.-J. Hwang, Synthesis of dihydroxylated chalcone derivatives with diverse substitution patterns and their radical scavenging ability toward DPPH free radicals, Bull. Korean Chem. Soc. 29 (2008) 1125–1130.
[28] J. Mai, E. Hoxha, C.E. Morton, B.M. Muller, M.J. Adler, Towards a dynamic covalent molecular switch: substituent effects in chalcone/flavanone isomerism, Org. Biomol. Chem. 11 (2013) 3421–3423.
[29] M.S. Thomsen, J.D. Mikkelsen, Type I and II positive allosteric modulators differentially modulate agonist-induced up-regulation of α7 nicotinic acetylcholine receptors, J. Neurochem. 123 (2012) 73–83.
[30] J.H. Grønlien, M. Håkerud, H. Ween, K. Thorin-Hagene, C.A. Briggs, M. Gopalakrishnan, J. Malysz, Distinct profiles of alpha 7 nAChR positive allosteric modulation revealed by structurally diverse chemotypes, Mol. Pharmacol. 72 (2007) 715–724.
[31] P. Perjési, M. Takács, E. Ösz, Z. Pintér, J. Vámos, K. Takács-Novák, In-solution and on-plate light-Catalyzed *E/Z* isomerization of Cyclic chalcone analogues. Lipophilicity of *E*- and *Z*-2-(X-Benzylidene)-1-Benzosuberones, J. Chromatogr. Sci. 43 (2005) 289–295.
[32] S. Iwata, T. Nishino, H. Inoue, N. Nagata, Y. Satomi, H. Nishino, S. Shibata, Antitumorigenic activities of chalcones (II). Photo-isomerization of chalcones and the correlation with their biological activities, Biol. Pharm. Bull. 20 (1997) 1266–1270.
[33] J. Malysz, J.H. Grønlien, D.J. Anderson, M. Håkerud, K. Thorin-Hagene, H. Ween, C. Wetterstrand, C.A. Briggs, R. Faghih, W.H. Bunnelle, M. Gopalakrishnan, In vitro pharmacological characterization of a novel allosteric modulator of α7 neuronal acetylcholine receptor, 4-(5-(4-chlorophenyl)-2-methyl-3-propionyl-1*H*-pyrrol-1-yl)benzenesulfonamide (A-867744), exhibiting unique pharmacological profile, J. Pharm. Exp. Ther. 330 (2009) 257–267.
[34] J. Amanaganti, N.J.P. Subhashini, Potential biological activity of chalcones: a review, J. Chem. Sci. 11 (2013) 1335–1341.
[35] L. Wu, M.H.N. Ashraf, M. Facci, R. Wang, G. Phyllis, P.G. Paterson, A. Ferrie, B.H.J. Juurlink, Dietary approach to attenuate oxidative stress, hypertension, and inflammation in the cardiovascular system, Proc. Natl. Acad. Sci. U S A 101 (2004) 7094–7099.
[36] J. Egea, A.O. Rosa, A. Cuadrado, A.G. Garcia, M.G. Lopez, Nicotinic receptor activation by epibatidine induces heme oxygenase-1 and protects chromaffin cells against oxidative stress, J. Neurochem 102 (2007) 1842–1852.
[37] J. Liu, L. Li, W.Z. Suo, HT22 hippocampal neuronal cell line possesses functional cholinergic properties, Life Sci. 84 (2009) 267–271.
[38] E. Parada, J. Egea, A. Romero, L. del Barrio, A.G. García, M.G. López, Poststress treatment with PNU-282987 can rescue SH-SY5Y cells undergoing apoptosis via α7 nicotinic receptors linked to a Jak2/Akt/HO-1 signaling pathway, Free Radic. Biol. Med. 49 (2010) 1815–1821.
[39] E. Parada, J. Egea, I. Buendia, P. Negredo, A.C. Cunha, S. Cardoso, M.P. Soares, M.G. López, The microglial α7-acetylcholine nicotinic receptor is a key element in promoting neuroprotection by inducing heme oxygenase-1 via nuclear factor erythroid-2-related factor 2, Antioxid. Redox Signal 19 (2013) 1135–1148.
[40] R. Roncarati, C. Scali, T.A. Comery, S.M. Grauer, S. Aschmi, H. Bothmann, B. Jow, D. Kowal, M. Gianfriddo, C. Kelley, U. Zanelli, C. Ghiron, S. Haydar, J. Dunlop, G.C. Terstappen, Procognitive and neuroprotective activity of a novel alpha7 nicotinic acetylcholine receptor agonist for treatment of neurodegenerative and cognitive disorders, J. Pharmacol. Exp. Ther. 329 (2009) 459–468.
[41] S. Suzuki, J. Kawamata, T. Matsushita, A. Matsumura, S. Hisahara, K. Takata, Y. Kitamura, W. Kem, S. Shimohama, 3-[(2,4-Dimethoxy)benzylidene]-anabaseine dihydrochloride protects against 6-hydroxydopamine-induced parkinsonian neurodegeneration through α7 nicotinic acetylcholine receptor stimulation in rats, J. Neurosci. Res. 91 (2013) 462–471.
[42] L. Del Barrio, M.D. Martín-de-Saavedra, A. Romero, E. Parada, J. Egea, J. Avila, J.M. McIntosh, S. Wonnacott, M.G. López, Neurotoxicity induced by okadaic acid in the human neuroblastoma SH-SY5Y line can be differentially prevented by α7 and β2* nicotinic stimulation, Toxicol. Sci. 123 (2011) 193–205.
[43] H.V. Nobre-Júnior, R.A. Oliveira, F.D. Maia, M.A. Nogueira, M.O. de Moraes, M.A. Bandeira, G.M. Andrade, G.S. Viana, Neuroprotective effects of chalcones from Myracrodruon urundeuva on 6-hydroxydopamine-induced cytotoxicity in rat mesencephalic cells, Neurochem. Res. 34 (2009) 1066–1075.
[44] G. Munro, R. Hansen, H. Erichsen, D. Timmermann, J. Christensen, H. Hansen, The alpha7 nicotinic ACh receptor agonist compound B and positive allosteric modulator PNU-120596 both alleviate inflammatory hyperalgesia and cytokine release in the rat, Br. J. Pharmacol. 167 (2012) 421–435.
[45] K. Freitas, F.I. Carroll, M.I. Damaj, The antinociceptive effects of nicotinic receptors alpha7-positive allosteric modulators in murine acute and tonic pain models, J. Pharmacol. Exp. Ther. 344 (2013) 264–275.
[46] K. Freitas, S.S. Negus, F.I. Carroll, M.I. Damaj, In vivo pharmacological interactions between a type II positive allosteric modulator of alpha7 nicotinic ACh receptors and nicotinic agonists in a murine tonic pain model, Br. J. Pharmacol. 169 (2013) 567–579.
[47] Y. Nagakura, M. Okada, A. Kohara, T. Kiso, T. Toya, I. Akihiko, F. Wanibuchi, T. Yamaguchi, Allodynia and hyperalgesia in adjuvant-induced arthritic rats: time course of progression and efficacy of analgesics, J. Pharmacol. Exp. Ther. 306 (2003) 490–497.

[48] S. Sogawa, Y. Nihro, H. Ueda, A. Izumi, T. Miki, H. Matsumoto, T. Satoh, 3,4-Dihydroxychalcones as potent 5-lipoxygenase and cyclooxygenase inhibitors, J. Med. Chem. 36 (1993) 3904–3909.
[49] H.K. Hsieh, T.H. Lee, J.P. Wang, J.J. Wang, C.N. Lin, Synthesis and anti – inflammatory effect of chalcones and related compounds, Pharm. Res. 15 (1998) 39–46.
[50] S.L. McLean, N. Idris, B. Grayson, D. Gendle, C. Mackie, A. Lesage, D.J. Pemberton, J. Neill, PNU-120596. a positive allosteric modulator of α7 nicotinic acetylcholine receptors, reverses a sub-chronic phencyclidine-induced cognitive deficit in the attentional set-shifting task in female rats, J. Psychopharmacol. 26 (2012) 1265–1270.
[51] M. Criado, L.M. Valor, J. Mulet, S. Gerber, S. Sala, F. Sala, Expression and functional properties of α7 acetylcholine nicotinic receptors are modified in the presence of other receptor subunits, J. Neurochem 123 (2012) 504–514.
[52] N. Dominguez, M. Rodriguez, J.D. Machado, R. Borges, Preparation and culture of adrenal chromaffin cells, Methods Mol. Biol. 846 (2012) 223–234.
[53] J.D. Machado, M.S. Montesinos, R. Borges, Good practices in single cell amperometry, Methods Mol. Biol. 440 (2008) 297–313.
[54] F. Segura, M.A. Brioso, J.F. Gomez, J.D. Machado, R. Borges, Automatic analysis for amperometrical recordings of exocytosis, J. Neurosci. Methods 103 (2000) 151–156.
[55] T. Mosmann, Rapid colorimetric assay for cellular growth and survival application to proliferation and cytotoxicity assays, J. Immunol. Methods 65 (1983) 55–63.
[56] F. Denizot, R. Lang, Rapid colorimetric assay for cell growth and survival. Modifications to the tetrazolium dye procedure giving improved sensitivity and reliability, J. Immunol. Methods 89 (1986) 271–277.
[57] C. García-Martínez, A. Fernández-Carvajal, B. Valenzuela, A. Gomis, W. Van Den Nest, S. Ferroni, C. Carreño, C. Belmonte, A. Ferrer-Montiel, Design and characterization of a noncompetitive antagonist of the transient receptor potential vanilloid subunit 1 channel with in vivo analgesic and anti-inflammatory activity, J. Pain 7 (2006) 735–746.
[58] C.V. Vorhees, M.T. Williams, Morris water maze: procedures for assessing spatial and related forms of learning and memory, Nat. Protoc. 1 (2006) 848–858.
[59] D. Pereda, M.R. Pardo, Y. Morales, N. Dominguez, M.R. Arnau, R. Borges, Phenotypic characterization of mice lacking chromogranins. (Unpublished results).